The effect of the interplay between PGC-1α and HIF-1α on preserving mitochondrial metabolism in diabetic kidney disease

Lee, Jee Young

Department of Medicine
Graduate School
Yonsei University

The effect of the interplay between PGC-1α and HIF-1α on preserving mitochondrial metabolism in diabetic kidney disease

Advisor Han, Seung Hyeok

A Dissertation Submitted
to the Department of Medicine
and the Committee on Graduate School
of Yonsei University in partial fulfillment of the
Requirements for the Degree of
Doctor of Philosophy in Medical Science

Lee, Jee Young

June 2025

The effect of the interplay between PGC-1α and HIF-1α on preserving mitochondrial metabolism in diabetic kidney disease

This Certifies that the Dissertation of Lee, Jee Young is Approved

Committee Chair	Park, Jung Tak
Committee Member	Han, Seung Hyeok
Committee Member	Lim, Beom Jin
Committee Member	Yu, Je-Wook
Committee Member	Kim, Hyoungnae

Department of Medicine
Graduate School
Yonsei University
June 2025

ACKNOWLEDGEMENTS

I am deeply thankful to my thesis supervisor and mentor, Professor Seung Hyeok Han, for guiding me with his intellectual insights and belief in me. His guidance has led me to pursue my dream of becoming a specialist in nephrology. Without his support, I would not be where I am today.

I would also like to express my gratitude to Professor Shin-Wook Kang. The foundation for the Institute of Kidney Disease, College of Medicine, Yonsei University prospered through his dedication and efforts. Thanks to his devotion to the Institute of Kidney Disease, I was able to pursue this Master of Medical Science degree. I want to express my gratefulness to the thesis committee members—Professors Jung Tak Park, Beom Jin Lim, Je-Wook Yu, and Hyoungnae Kim—who have provided professional advice that led to the successful completion. I am grateful to Professor Tae-Hyun Yoo, who taught me much about research and treatment in nephrology when I was taking my first steps as a trainee. I am also deeply grateful to Professor Young Su Joo; I cannot thank him enough for all the assistance and guidance he has provided throughout my career. I would also like to thank Bo Young Nam for all the uncountable support she has shown me throughout my doctoral dissertation. I also thank Gyuri Kim, Yoo Jin Cho, Ju Yeon Park, and Jaejin Ryu for their efforts and technical support. They helped me every step of the way in my experimentation. I also want to express my appreciation to Ms. Hyojung Um for her kind support throughout my research.

Finally, I express my deep and sincere gratitude to my husband for his love, encouragement, and wisdom, which have guided me ever since I met you. I feel incredibly lucky to have found you. I also want to express my love and gratitude to my two beautiful daughters, who bring so much joy and love into my life. Although I did not mention everyone here, I am deeply grateful to all those I have encountered in my life. Together, they make life not only bearable but also worth living.

TABLE OF CONTENTS

LIST OF FIGURES

LIST OF TABLES

ABSTRACT

The effect of interplay between PGC-1α and HIF-1α on preserving mitochondrial metabolism in diabetic kidney disease

Background: Hypoxia-inducible factor-1α (HIF-1α) plays a multifaceted function in energy metabolism by promoting glycolysis and inhibiting the activity of pyruvate kinase M2 (PKM2). In contrast, peroxisome proliferator-activated receptor gamma coactivator-1α (PGC-1α) is a central regulator of mitochondrial biogenesis and oxidative energy production. I aimed to investigate how PGC-1α influences HIF-1α–mediated regulation of mitochondrial metabolism in renal tubular epithelial cells (RTECs) under diabetic conditions.

Methods: Primary RTECs from the C57BL/6 mice were high glucose (HG)-stimulated, with or without transfection using *Ppargc1a* plasmid (pPGC1α) or *Ppargc1a* small interfering RNA (siPGC1α) plasmid. Primary cultured RTECs were also exposed to succinate with or without pPGC1α or siPGC1α. To evaluate whether PGC-1α directly regulates HIF-1α, Chromatin immunoprecipitation (ChIP) and luciferase reporter assays were performed. *In vivo*, *db/db* mice were given daily doses of metformin or resveratrol daily via oral gavage for 12 weeks. We examined TCA cycle intermediates, PGC-1α, HIF-1α, PKM2 activity, glycolysis, fatty acid oxidation (FAO), and mitochondrial function and morphology.

Results: HG-treated RTECs exhibited decreased *Ppargc1a* and *Pkm2* expression, increased *Hif1a* expression, and shift toward aberrant glycolysis and impaired FAO. The defective metabolic alterations resulted in increased succinate levels, a key intermediate of TCA cycle. *Ppargc1a* overexpression reversed these changes, while silencing *Ppargc1a* exacerbated them. Succinate treatment in RTECs increased *Hif1a* expression but decreased *Pkm2* expression along with induced aberrant glycolysis. These changes were mitigated by silencing *Hif1a*. Chip assay results indicated direct binding of PGC-1α at the *Hif1a* promoter regulatory region. Regulatory action of *Ppargc1a* on *Hif1a* was inhibited under succinate exposure and potentiated by *Ppargc1a* overexpression. In an animal diabetic kidney disease study, *Ppargc1a* activation with metformin and resveratrol partially recapitulated the *in vitro* findings, showing favorable metabolic effects.

Conclusions: PGC-1α deficiency under diabetic conditions led to the accumulation of TCA cycle

intermediates, which enhanced HIF-1α activity and disrupted mitochondrial energy metabolism. Additionally, PGC-1α directly suppressed HIF-1α activity, elucidating its regulatory role in mitochondrial energy metabolism.

Key words : PGC-1α, HIF-1α, PKM2, TCA cycle, renal tubular epithelial cells, diabetic kidney disease

1. Introduction

With its increasing prevalence, chronic kidney disease (CKD) is a growing public health challenge worldwide. Approximately 14% of United States adults were presumed to have CKD in 2023 [1]. Depending on various factors, approximately 10-40% of patients with CKD may advance to end stage kidney disease (ESKD), which require life supporting renal replacement therapies such as dialysis or transplantation. In the US, ESKD affects 786,000 people and has a high mortality rate of nearly 50% within five years. Diabetic nephropathy is the foremost cause of ESKD, followed by hypertensive nephropathy as the second most common cause. The economic burden of CKD, ESKD, and associated comorbidities is substantial, accounting for almost 23% of Medicare fee-for-service [2]. Therefore, preventing CKD is crucial for reducing healthcare costs and complications, improving quality of life, and reducing mortality.

Among all organs, the kidney ranks as one of the most metabolically active and, at rest, is the second-largest consumer of oxygen in the body [3, 4]. Therefore, the kidney requires substantial energy to sustain essential functions such as waste excretion, electrolyte balance, and acid-base homeostasis [5-7]. To meet this high energy demand, renal tubular epithelial cells (RTECs) exhibit high mitochondrial density and primarily rely on oxidative phosphorylation for ATP production [8]. Proximal tubular cells in particular, are rich in mitochondria because reabsorption of glucose and sodium requires a significant amount of energy. The proximal tubule primarily utilizes fatty acids, lactate, and glutamine as its major fuel sources; however, the predominant energy substrate varies across different segments of the nephron. Consequently, diabetic kidney disease (DKD) pathogenesis is strongly linked to mitochondrial dysfunction [9-11].

Under physiological conditions, ATP is produced through aerobic glycolysis, where glucose is metabolized to pyruvate, which then enters the tricarboxylic acid (TCA) cycle to fuel oxidative phosphorylation. However, under hypoxic conditions, anaerobic glycolysis occurs, where pyruvate is transformed to lactate, leading to inefficient ATP production compared to aerobic glycolysis [12, 13]. Notably, in pathologic conditions such as DKD or cancer, cells increasingly rely on anaerobic glycolysis, leading to inefficient ATP production and a metabolic shift known as the Warburg effect [11, 14-18]. This shift is associated with increased lactate production, impaired mitochondrial metabolism, and cellular dysfunction. Therefore, RTECs under physiological condition, gluconeogenesis is favored over glycolysis. However, in RTECs of DKD energy generation shifts from aerobic glycogenesis to anaerobic glycolysis in which pyruvate transforms into lactate, which is then further metabolized by lactate dehydrogenase, leading to insufficient ATP generation.

Peroxisome proliferator-activated receptor-gamma coactivator-1α (PGC-1α) is essential for mitochondrial biogenesis and oxidative metabolism [19, 20]. It is a coactivator for DNA-binding transcription factors such as estrogen-related receptor, peroxisome proliferator-activated receptor α

/β, and nuclear respiratory factor 1/2. PGC-1α regulates genes related to oxidative phosphorylation and fatty acid oxidation (FAO) [21]. Notably, reduced PGC-1α activity has been observed in DKD models, contributing to mitochondrial dysfunction and kidney fibrosis [22, 23]. Conversely, pharmacological activators such as resveratrol and metformin have been shown to enhance PGC-1α function, thereby improving mitochondrial health and metabolic homeostasis [24, 25].

Hypoxia-inducible factor-1α (HIF-1α) is a crucial promotor of glycolysis and a transcriptional regulator involved in the cellular response to hypoxia. It regulates glucose transporters and glycolytic pathway enzymes expression, including pyruvate kinase M2 (PKM2), which has a crucial role in metabolic reprogramming [26-35]. PKM2 not only interacts with HIF-1α but also serves as its coactivator, enhancing the activation of HIF-1α target genes [26, 32]. Furthermore, HIF-1α also mediates the suppression of oxidative phosphorylation by activating pyruvate dehydrogenase kinase (PDK), which impairs the transformation of pyruvate into acetyl-CoA, further enhancing anaerobic glycolysis [36, 37]. Under hypoxic conditions, TCA cycle activity is reduced, leading to an increase in TCA cycle intermediates such as succinate, fumarate, which decreases the level of prolyl hydroxylase (PHD), an enzyme responsible for degrading HIF-1α, ultimately leading to its stabilization and prolonged activity [38].

Previous studies demonstrated that HIF-1α suppress PGC-1α activity in the kidney as well as the liver [39-41]. Qi et al. reported that in podocytes of DKD, activation of PKM2 with TEPP-46 enhanced PGC-1α function and reversed impaired mitochondrial metabolism [42]. To further evaluate how HIF-1α and PGC-1α interact at the molecular level, our group previously demonstrated that HIF-1α directly regulates PGC-1α with its regulation influenced by the level of PKM2 [43]. In this study, I hypothesized a reverse mechanism in which PGC-1α modulates HIF-1α to regulate mitochondrial metabolism in DKD. This study aimed to elucidate the mechanistic interactions between these key metabolic regulators, providing novel insights into the metabolic dysregulation underlying DKD.

2. MATERIALS AND METHODS

1. Primary renal tubular epithelial cell culture and gene transfection

RTECs from the kidneys of C57BL/6 mice were isolated. Extracted kidneys were chopped into pieces of approximately 1 mm^3 per 1 ml of icy Dulbecco's Phosphate-Buffered saline (DPBS) (Thermo Fisher Scientific, USA). Tissue fragments were incubated at 37°C for 30 minutes in a collagenase solution (1mg/mL in DPBS; Sigma-Aldrich, USA). Then, dissociate the tissues by vigorous pipetting to make a cell suspension. Afterwards, I filtered the supernatants using a 100-μm pore-sized nylon filter, then centrifugation at 3000 rpm for a duration of 10 minutes. The pellet was resuspended in sterile red blood cell lysis buffer (1 g $KHCO_3$, 8.26 g NH_4Cl, 0.037 g EDTA in 1L

of double-distilled H_2O) and incubated on ice for 10 minutes. Thereafter, it was subjected to centrifugation for 10 minutes at 3000 rpm. Resulting pellet was gently rinsed two times with DPBS and subsequently plated in tissue culture dishes with a diameter of 10cm. RTECs were cultured in Dulbecco's Modified Eagle Medium (DMEM) supplemented with 2.5 μg/mL amphotericin B (Sigma-Aldrich, USA), 100 U/mL Penicillin G (Sigma-Aldrich, USA), 10% fetal bovine serum (FBS) (Thermo Fisher Scientific, USA), and 20 ng/mL of epidermal growth factor (Sigma-Aldrich, USA). Once the RTECs reached approximately 70% confluence, they were serum-starved in low-glucose (LG) medium for 24 hours. In LG-RTECs (control group), the medium was replaced with DMEM containing 1% FBS. The high-glucose (HG)-RTECs experimental group was treated with 1% FBS-DMEM and 40 mM D-glucose to simulate the hyperglycemic environment characteristic of diabetic kidney disease (DKD). RTECs were harvested 48 hours after the media change.

Primary cultured RTECs were exposed to HG with empty vector or scrambled small interfering RNA (siRNA) or *Ppargc1a* plasmid (pPGC1α) or Ppargc1a siRNA (siPGC1α). In *Hif1a*-knockdown experiments, I transfected RTECs with scrambled siRNA or mouse *Hif1a* siRNA (siHIF1α) with Lipofectamine RNAiMAX reagents (Invitrogen, USA). Subsequently, the cells were stimulated with either HG or succinate for an additional 48 hours and subsequently analyzed.

2. Animal study and treatment

For the animal study, B6.Cg-M+/+Lepr^{db}/Lepr^{db} (*db/db*) mice and B6.Cg-M+/-Lepr^{db}/$^{+}$ (*db/m*) mice were used (Jackson Laboratories, USA). As the experimental model for DKD, *db/db* mice were used and *db/m* mice serving as non-diabetic controls. The experimental and control groups each consisted of 3 subgroups, with 5 mice in each subgroup. Within the 3 groups, the first group was given only diets and water, the second group was given metformin, and the last group was given resveratrol. Metformin (200 mg/kg/day) and resveratrol (20mg/kg/day) were given daily via gavage for 12 weeks from 7 weeks of age. Diets and water were provided ad libitum. After 12 weeks, kidneys were surgically removed under anesthesia using a combination of 10 mg per kg of Zoletil (Virbac, France) and 10mg per kg of Rompune via intraperitoneal injection. After sacrifice, kidney samples were quickly snap-frozen in liquid nitrogen, then stored at -80°C for further use. Urine for measuring 24-hour albuminuria was collected in the metabolic monitoring cages and analyzed at euthanasia. Glucometer was used to measure blood glucose, and Albuwell M kit enzyme-linked immunosorbent assay kit (Exocell, USA) was used to measure 24-hour urinary albumin. The experimental protocols for animals were authorized through the Committee for the Care and Use of Laboratory Animals at Yonsei University College of Medicine (Seoul, Republic of Korea). Animal procedures were carried out following the Principles of Laboratory Animal Care (NIH Publication no. 85–23, revised 1985).

3. RNA extraction

The RTEC cell culture dishes were added with RNAiso reagent (700 μL; Takara Bio Inc., Japan). The cell suspensions were gathered and mixed at room temperature (RT) for 5 minutes. The whole mouse kidney specimens were frozen instantly with liquid nitrogen and homogenized 3 times with 700 μL RNAiso reagent using mortar and pestle. Then, 160 uL chloroform was applied to the homogenized RTECs and kidney specimens. The specimens were then mixed thoroughly for 30 seconds, incubated at RT for 3 minutes, and centrifuged at 12,000 rpm for 15 minutes at 4℃. Samples from the upper layer of the three-phase separation, of the aqueous phase were transferred to a fresh tube and precipitated using 400 μL of isopropanol. The mixture was granulated by centrifugation at 12,000 rpm for 30 minutes at 4°C. Thereafter, the RNA precipitate was rinsed using 70% ethanol, left to dry for 2 minutes, then dissolved in diethyl pyrocarbonate (DEPC)-treated sterile distilled water. The quantity and purity of the RNA were assessed by spectrophotometric measurements at 260/280 nm.

4. Reverse RNA transcription

First-strand complimentary DNA (cDNA) corresponding to the obtained RNA was synthesized using the cDNA synthesis kit (Takara Bio Inc, Japan). 2 micrograms of total RNA were reverse transcribed using a reaction mixture containing 10 μM random hexanucleotide primer, 30 mM KCl, 8 mM $MgCl_2$, 1mM dNTP, 50 mM Tris-HCl (pH 8.5), 0.2 mM dithiothreitol, 25 U RNase inhibitor, and 40 U PrimeScript reverse transcriptase. The solution was incubated at 30℃ for 10 minutes, then at 42℃ for 1 hour. Then, subsequently heated to 99℃ for 5 minutes to deactivate the enzyme.

5. Real-time quantitative PCR

Polymerase chain reaction (PCR) was performed using the ABI PRISM 7700 Sequence Detection System (Applied Biosystems, USA). PCR was carried out in a total reaction volume of 20-μL, consisting of 5 μL cDNA template, 5 pM each of forward and reverse primers (Applied Biosystems, USA), and 10 μL of SYBR Green PCR Master Mix (Applied Biosystems, USA). The primers used for quantitative PCR are detailed in Table 1. PCR was conducted using the following cycling conditions: denaturation at 95°C for 9 minutes, 35 cycles of denaturation at 94.5℃ for 30 minutes, annealing at 60°C for 30 seconds, and extension at 72°C for 1 minute, with a final extension step at 72°C for 7 minutes. Each sample was analyzed in triplicate using separate tubes, with a no-cDNA control included in each assay. Following real-time PCR, melting curve analysis was performed by gradually increasing the temperature at a rate of 2°C/min from 60°C to 95°C. The cDNA levels for each specimen were quantified using the comparative CT method ($2^{-\Delta\Delta CT}$). Data are presented as relative expression normalized to 18S ribosomal RNA (rRNA) and expressed in arbitrary units. Data from the control group were assigned a baseline relative value of 1.0. I compared the transcription level of the following genes: *Ppargc1a, Hif1a, and Pkm2*; genes associated with glycolysis (*Glut1,*

Hk, *Pdha*, and *Ldha)*; genes involved in with FAO (*Cpt1* and *Acox1*); genes involved in the mitochondrial dynamics (*Mfn* and *Drp1*); genes related to apoptosis (*Bax* and *Bcl-2*); and genes associated with fibrosis (*Fn1*, and *Col1a1*).

Table 1. Primer sequences

Gene	Forward	Reverse
Ppargc1a	AGTCCCATACACAACCGCAG	CCCTTGGGGTCATTTGGTGA
Hif1a	GGATGAGTTCTGAACGTCGAAA	AATATGGCCCGTGCAGTGAA
Pkm2	TCGCATGCAGCACCTGATT	CCTCGAATAGCTGCAAGTGGTA
Glut1	ACACTCACCACGCTTTGGTC	ACACACCGATGATGAAGCGG
Hk	CCAAAATAGACGAGGCCGTA	TTCAGCAGCTTGACCACATC
Ldha	GCTCCCCAGAACAAGATTACAG	TCGCCCTTGAGTTTGTCTTC
Pdha	CAAAGTTTGCGGCTGCCTAT	GGTAGCGGTAAGTCTGGAGC
Sdha	CTCCTGCCTCTGTGGTTGAG	ACAGCTGAAGTAGGTTCGCC
Mfn	AACGCTCTCTCTTTCGCACG	TTGGAAAACAGTGGGCTGGA
Drp1	GCTGCCTCAGATCGTCGTAG	GGTGACCACACCAGTTCCTC
Acox1	CTTGGATGGTAGTCCGGAGA	TGGCTTCGAGTGAGGAAGTT
Cpt1	GGTCTTCTCGGGTCGAAAGC	TCCTCCCACCAGTCACTCAC
Fn	TGACAACTGCCGTAGACCTGG	TACTGGTTGTAGGTGTGGCCG
Col1a1	GCCAAGAAGACATCCCTGAA	GTTTCCACGTCTCACCATTG
Bax	TGCAGAGGATGATTGCTGAC	GATCAGCTCGGGCACTTTAG
Bcl-2	AGGAGCAGGTGCCTACAAGA	GCATTTTCCCACCACTGTCT
18s	CGCTTCCTTACCTGGTTGAT	GGCCGTGCGTACTTAGACAT

6) Western blot analysis

Protein production of PGC-1α, HIF-1α, and markers of the glycolysis, and FAO pathways, mitochondria biogenesis, mitochondrial dynamics, fibrosis, and apoptosis were measured using Western blot analyses. Cultured RTECs and kidneys were collected and processed with sodium dodecyl sulfate (SDS) sample buffer containing 2% SDS, 10 mM Tris·HCl (pH 6.8), and 10% (v/v) glycerol. After scraping adherent cells from the culture dish, the cell suspension was transferred to a microtube and then centrifuged at 10,000 rpm at 4℃ for 10 minutes. The supernatant was carefully removed by aspiration, and the pellet was discarded. The supernatant was moved to a fresh tube, then stored at -20°C. The BCA assay with a Bio-Rad kit was used to measure the protein concentrations of the lysates (Bio-Rad Laboratories, Inc., USA). I then mixed portions containing 50 μg of protein extracts with Laemmli sample buffer (2% SDS, 10 mM pH 6.8 Tris·HCl, and 10% (v/v) glycerol). The mixture was boiled for 5 minutes at 100°C and then subjected to electrophoresis on a 12% acrylamide denaturing SDS polyacrylamide gel. Thereafter, proteins were transported onto a Hybond-ECL membrane using a Hoefer semi-dry blotting apparatus (Hoefer Instruments, USA). The membrane was exposed to blocking buffer A (1× PBS, 0.1% Tween 20, and 5% nonfat milk) and incubated for 30 minutes at RT. Subsequently an overnight incubation was done at 4°C in a

1:1,000 dilution of polyclonal antibodies. The following primary antibodies used for analyzing the proteins of interest: PGC-1α (Abcam, USA), HIF-1α (Novus Biologicals, USA), carnitine palmitoyltransferase 1 (CPT1) (Novus Biologicals, USA), peroxisomal acyl-coenzyme A oxidase 1 (ACOX1) (Abcam, USA), type I collagen (COL1) (Southern Biotech, USA), fibronectin (FN) (DAKO, USA), B-cell lymphoma 2 (BCL-2) (Santa Cruz Biotechnology, USA), Bcl-2-associated X (BAX) (Santa Cruz Biotechnology, USA), dynamin related protein 1 (DRP1) (BD Biosciences, USA), mitofusin 1 (MFN1) (Cell Signaling Technology, USA), and β-actin (Sigma-Aldrich, USA). Thereafter, the membrane was rinsed for 15 min and then rinsed again for 5 min in 1× PBS with 0.1% Tween 20. Afterwards, the membrane was incubated with buffer A containing a 1:2,000 dilution of horseradish peroxidase-linked donkey anti-goat IgG (Santa Cruz Biotechnology, USA) as secondary antibody. The membrane was washed multiple times, then was developed using a chemiluminescent substrate (ECL; Amersham Life Science, USA). The band densities were measured (TINA image software, Germany) and the optical density changes in the bands of the treated groups compared to the control tissues and cells were calculated.

7) Measurement of succinate concentration

Succinate concentration was measured calorimetrically in tissue and cell extractions using standardized assay kits (ab204718, Abcam and ab102516, Abcam, respectively). Samples were placed into a 96-well plate, then the optical density at 450 nm was measured.

8) ChIP assay

The Chromatin immunoprecipitation (ChIP) was carried out following the method outlined in a prior publication. [44]. In short, primary culture cells were cross-linked, washed, then sonicated. Following lysis, samples were immunoprecipitated using either anti-mouse HIF-1α antibodies (Abcam, USA) or control IgG (Santa Cruz Biotechnology, USA). Immunoprecipitants were retrieved using Protein A agarose combined with Salmon sperm DNA (Millipore, USA). Bounded proteins were eluted following the wash steps, and ChIP-enriched DNA was isolated through phenol:chloroform extraction. The eluted ChIP DNA, along with input controls, was subjected to quantitative PCR using primers specific to the *Hif1a* enhancer/promoter region. Primer used in this study: sense, 5'-CAACGACCACCCACCCCA-3' and anti-sense, 5'-GTAGAAGAAAAAGACT CCTG-3'. As detailed in previous publication, data were corrected using input sample values. [44].

9) Luciferase Assay

The *Hif1a* promoter luciferase plasmid (pGL3-Hif-1α) and the empty vector control plasmid (pGL3-basic) were purchased from Addgene (USA). Primary RTECs were seeded in six-well plates and cultured during the night. The next day, cells were transfected with 400 ng of either pGL3-basic or pGL3–Hif-1α plasmid, along with 100 ng Renilla luciferase–encoding plasmid, using

Lipofectamine 2000, in accordance with the manufacturer's instructions. 24 hours after transfection we gathered and analyzed the cells using the Dual-Luciferase Reporter Assay System (E1910, Promega, USA). Luminescence measurements were performed with a CentroXS^3 LB9601 luminometer (Berthold Technologies, Germany). Luciferase activity was adjusted to the Renilla luciferase activity, and intergroup differences were expressed as relative fold changes.

10) Transmission electron microscopy

Mitochondrial architecture was investigated using standard transmission electron microscopy (JEOL 1010, Japan). Dissected kidney tissues and primary RTECs were rinsed with cold PBS (pH 7.4), fixed overnight in a solution containing 2.5% glutaraldehyde and 2% paraformaldehyde, then rinsed, dehydrated, and embedded within a resin matrix according to standardized protocol.

11) Histological staining

Periodic acid–Schiff (PAS) and Masson's trichrome staining were applied to 10% formalin-fixed, paraffin-embedded kidney sections to assess histological features. PAS staining was performed after deparaffinization of the tissue slides, followed by incubation at 60°C for more than 30 minutes. Then they were rehydrated with xylene, followed by 100%, 95%, and 90% ethanol. After rinsing the slides using distilled water, the slides were placed in periodic acid for 7 minutes and then exposed to Schiff's solution for 15 minutes. Counterstaining was carried out using modified Mayer's Hematoxylin counterstaining following the dehydration process. Masson trichrome (MT) staining was performed as follows: Segments paraffin-embedded tissues with thickness of 5μm were deparaffinized, rehydrated with ethyl alcohol, washed with tap water, and then re-fixed in Bouin's solution for 1 hour at 56°C. The samples were washed in running tap water for 10 minutes, then stained with Weigert's iron hematoxylin working solution for 10 minutes. Following this, they were treated with Biebrich scarlet-acid fuchsin solution for 15 minutes and rinsed again in tap water. The sections were differentiated in a phosphomolybdic-phosphotungstic acid solution for 15 minutes, followed by transfer to aniline blue solution for 10 minutes of staining. After a brief rinse in running water, the sections were treated with 1% acetic acid solution for 5 minutes. Images were analyzed by determining the percentage of positively stained areas (PAS: purple; MT: sky-blue and blue color) using the color-deconvolution plugin and measuring area fractions (Image-J, version 1.49, National Institutes of Health, USA; http://imagej.net/ij).

12) MitoSox stain

Mitochondrial ROS production was measured by soaking the cells in Hank's Balanced Salt Solution following certain treatments. Once certain procedures were completed, the cells were then stained 20 min at 37 °C with MitoSOX (Elanco, USA). Cellular fluorescence was measured using a

LSM 710 confocal microscopy (Carl Zeiss, Germany).

13) Data analysis

All experimental data were analyzed using GraphPad Prism 9.4 (GraphPad Software, USA) and are presented as mean ± standard deviation. I conducted a one-way analysis of variance (ANOVA), the Tukey test for multiple comparisons, and Student's t-test for pairwise comparisons. A p-value of less than 0.05 was considered statistically significant.

3. RESULTS

1. PGC-1α is a key regulator of mitochondrial energy metabolism in HG-RTECs

To examine the effects of HG exposure on mitochondrial energy metabolism, I first evaluated the transcriptional activity of key metabolic genes to understand their regulation. As expected, HG-RTECs exhibited decreased transcript expression of *Ppargc1a* and *Pkm2*, while *Hif1a* mRNA expression levels were elevated relative to the control group (Fig 1A-C). These alterations coincided with increased mRNA expression of glycolytic genes such as *Glut1, Hk,* and *Ldha*, along with decreased *Pdha* expression, suggesting a metabolic shift towards aberrant glycolysis (Fig 1D-G). Additionally, genes related to FAO including *Acox1* and *Cpt1* were downregulated in HG-RTECs, indicating impaired FAO (Fig 1H-I). To examine the role of PGC-1α in counteracting HG-induced metabolic dysfunction, I manipulated *Ppargc1a* expression in RTECs. Overexpression of *Ppargc1a* (pPGC1α) significantly decreased transcript levels of *Hif1a*, restored *Pkm2* expression, and reversed the HG-induced alterations in glycolytic flux-related genes (Fig 1A-C). Additionally, impaired level of FAO related genes in HG-RTECs were restored upon *Ppargc1a* overexpression (Fig 1H-I). The protein levels of PGC-1α, HIF-1α, CPT1, and ACOX1 showed the same trend as the mRNA levels under HG treatment and *Ppargc1a* overexpression (Fig 1J).

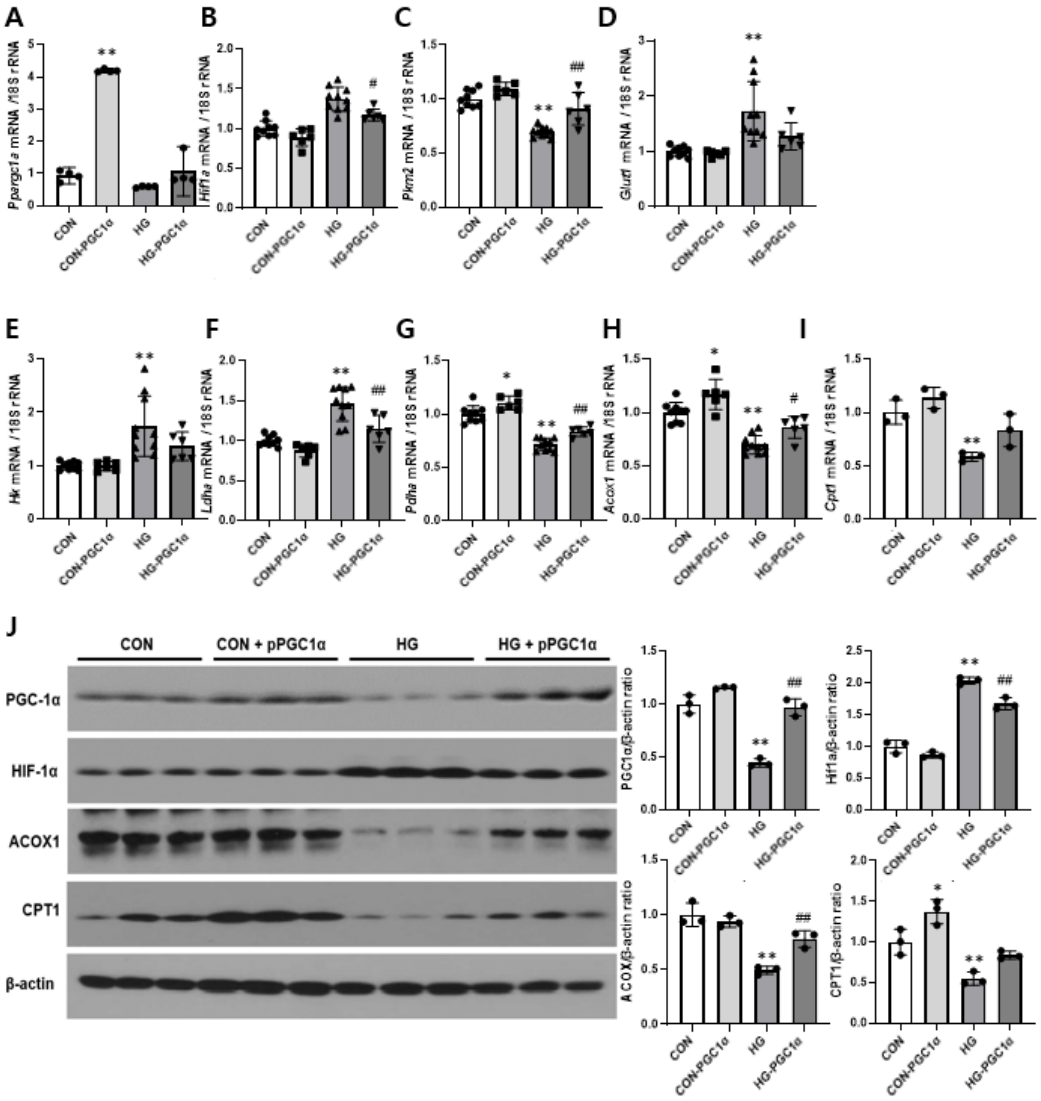

Fig 1. *Ppargc1a* overexpression restores altered energy metabolism and mitochondrial dysfunction in HG-RTECs. Primary RTECs were transfected with *Ppargc1a* plasmid (pPGC1α) or vector plasmid and 40 mM glucose for 48 hours. (A) The *Ppargc1a* mRNA expression level was decreased in HG-RTECs, and this reduction was further diminished by *Ppargc1a* overexpression. (B) The *Hif1a* mRNA expression level was elevated in HG-RTECs, and this increase was reversed by *Ppargc1a* overexpression. (C) The mRNA level of *Pkm2* was decreased in HG-RTECs, but this reduction was reversed by pPGC1α transfection. (D-G) The mRNA levels of the aberrant glycolysis pathway were increased in HG-RTECs, which were decreased by pPGC1α addition. (H-I) The mRNA level of *Cpt1* and *Acox1* were reduced in HG-RTECs and reversed by pPGC1α. (J) Protein levels of PGC-1α, CPT1, and ACOX1 were reduced and HIF-1α was increased in HG-RTECs. Data (n = 10 per group): mean ± standard error of the mean * p <0.05, ** p <0.01 (versus control group

(CON)); $^{\#}p$ <0.05, $^{\#\#}p$ <0.01 (versus HG)

Conversely, silencing *Ppargc1a* (siPGC1α) effectively downregulated *Ppargc1a,* accompanied by decreased *Pkm2* expression and increased *Hif1a* expression (Fig 2A-C). These changes exacerbated metabolic disruptions, leading to further activation of glycolytic genes thereby activating aberrant glycolysis, and worsening FAO impairment (Fig 2D-I). The protein level of PGC-1α, HIF-1α, and FAO markers exhibited a similar pattern to the mRNA levels under the HG environment and *Ppargc1a* overexpression (Fig 2J). These findings support the essential role of PGC-1α within mitochondrial energy metabolism, mitigating the metabolic dysfunction induced in HG-RTECs.

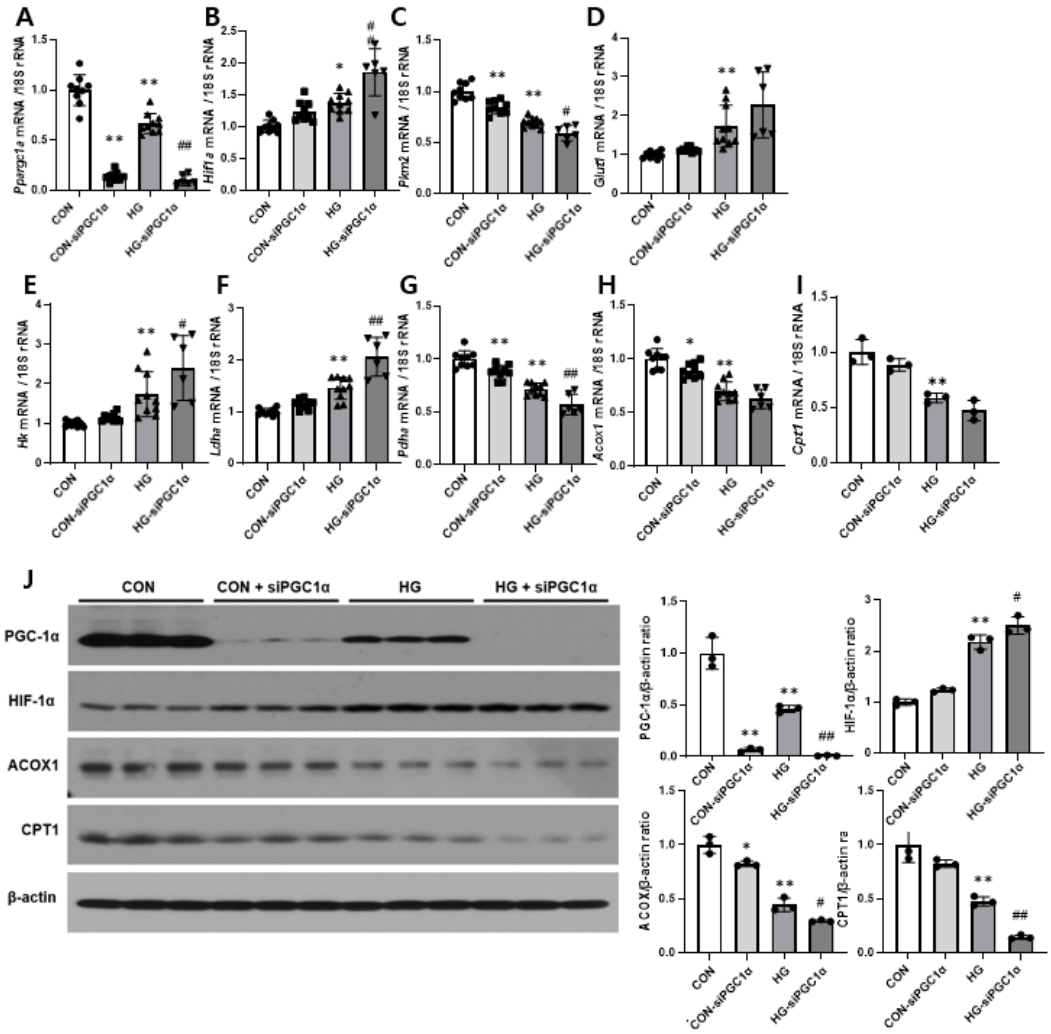

Fig 2. Silencing *Ppargc1a* in HG-RTECs reduces PKM2 activity, induces aberrant glycolytic flux, and suppresses fatty acid oxidation. Primary RTECs were transfected with *Ppargc1a* small interfering RNA (siPGC1α) or vector plasmid and 40 mM glucose for 48 hours. (A) The mRNA level of *Ppargc1a* was reduced in HG-RTECs, an effect that was aggravated by siPGC1α plasmid transfection. (B) The mRNA transcription level of *Hif1a* was increased in HG-RTECs, which was aggravated by *Ppargc1a* silencing. (C) The mRNA level of *Pkm2* decreased in HG-RTECs, a change that was aggravated by siPGC1α plasmid transfection. (D-G) The mRNA levels of aberrant glycolysis pathways in HG-RTECs were elevated and further aggravated by the transfection of siPGC1α (H-I) The mRNA transcription level of *Cpt1* and *Acox1*, the markers of FAO, were reduced in HG-RTECs, an effect that was further decreased by siPGC1 α addition. (J) The protein levels of PGC-1α, ACOX1, and CPT1 were decreased, while HIF-1α were elevated in HG-RTECs. These results were reversed by adding siPGC1α . Data (n = 10 per group): mean ± standard error of the mean * p <0.05, ** p <0.01 (versus control group (CON)); $^{\#}$ p <0.05, $^{\#\#}$ p <0.01 (versus HG)

2. PGC-1α modulates TCA cycle intermediates and prevents succinate accumulation

Previous studies using PGC-1α knockout mice have demonstrated significant downregulation of multiple TCA cycle genes, including succinate dehydrogenase complex flavoprotein subunit A (*Sdha*) [52-54]. The loss of these enzymes leads to the accumulation of succinate. Notably, succinate stabilizes HIF-1α by inhibiting PHD [55-57]. Given the substantial decrease in PGC-1α expression following HG exposure, I next investigated the mRNA expression levels of *Sdha*, a TCA enzyme, along with the accumulation of the TCA intermediate succinate in HG-RTECs (Fig 3A). HG exposure significantly decreased *Sdha* expression levels in contrast to the control group. These outcomes were concordant to increased succinate level (Fig 3B). Overexpression of *Ppargc1a* restored *Sdha* expression and significantly reduced the accumulation of succinate. Conversely, silencing *Ppargc1a* with siRNA further suppressed *Sdha* expression and exacerbated the accumulation of succinate (Fig 3C-D). These findings suggest that PGC-1α is essential for preserving TCA cycle stability, preventing excess succinate accumulation, and subsequently modulating HIF-1α activity.

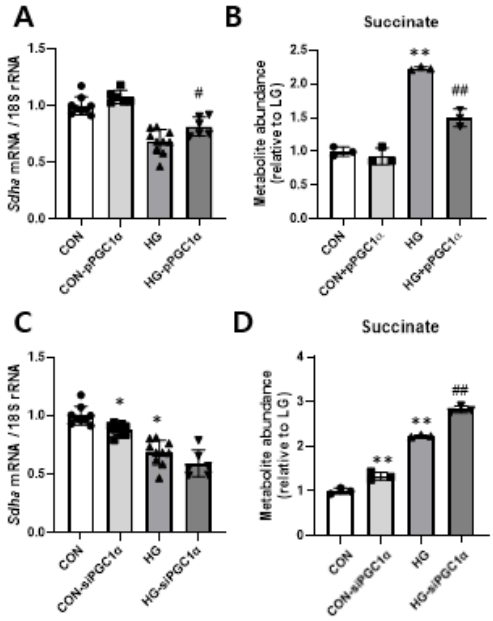

Fig 3. PGC-1α regulates succinate accumulation in HG-RTECs.
(A) The mRNA of the succinate dehydrogenase complex flavoprotein subunit A (*Sdha*) is decreased in HG-RTEC and increased by *Ppargc1a* overexpression. (B) Succinate, an intermediate of the TCA cycle is increased with HG-treatment and attenuated with the addition of *Ppargc1a* plasmid (pPGC1 α). (C) *Sdha* mRNA is attenuated with *Ppargc1a* silencing. (D) Succinate is increased with the addition of small interfering RNA (siPGC1α) plasmid. Data (n = 10 per group): mean ± standard error of the mean * p <0.05, ** p <0.01 (versus control group (CON)); $^{\#}p$ <0.05, $^{\#\#}p$ <0.01 (versus HG)

3. PGC-1α indirectly regulates HIF-1α by modulating succinate, promoting aberrant glycolysis, and decreasing fatty acid oxidation

To further examine the link between succinate accumulation and HIF-1α activation, I analyzed the expression levels of *Hif1a* and its downstream metabolic regulators in succinate-treated RTECs. Succinate exposure significantly increased *Hif1a* mRNA expression and upregulated glycolytic flux genes, including *Hk, Pdha*, and *Ldha* (Fig 4A-D). These findings suggest that succinate serves as a metabolic signal to enhance HIF-1α activity, promoting glycolysis at the expense of oxidative metabolism.

To determine whether HIF-1α directly mediates these metabolic alterations, I silenced *Hif1α* in succinate-treated RTECs. *Hif1a* knockdown effectively reversed the succinate-induced changes, reducing *Hk, Pdha*, and *Ldha* expression (Fig 4A-D). These results indicate that HIF-1α activation, driven by succinate accumulation, plays a pivotal role in reprogramming glucose metabolism

towards aberrant glycolysis. Succinate addition significantly decreased *Sdha* level, and silencing *Hif1a* with siRNA increased *Sdha* expression (Fig 4E). Additionally, I explored the function of HIF-1α in regulating PKM2, a key enzyme controlling the balance between aerobic and anaerobic glycolysis. *Hif1a* silencing restored *Pkm2* expression, suggesting that HIF-1α suppresses PKM2 activity, thereby reinforcing the metabolic shift towards inefficient glycolysis (Fig 4F). Furthermore, *Hif1a* knockdown restored FAO-associated gene expression, indicating that succinate-induced HIF-1α activation contributes to metabolic inflexibility in HG-RTECs (Fig 4G-H). Protein levels of HIF-1α and markers of FAO exhibited a comparable trend to the mRNA levels with succinate addition and *Hif1a* silencing (Fig 4I). Collectively, PGC-1α indirectly regulates HIF-1α activation by modulating succinate levels, which in turn regulates metabolic reprogramming towards glycolysis.

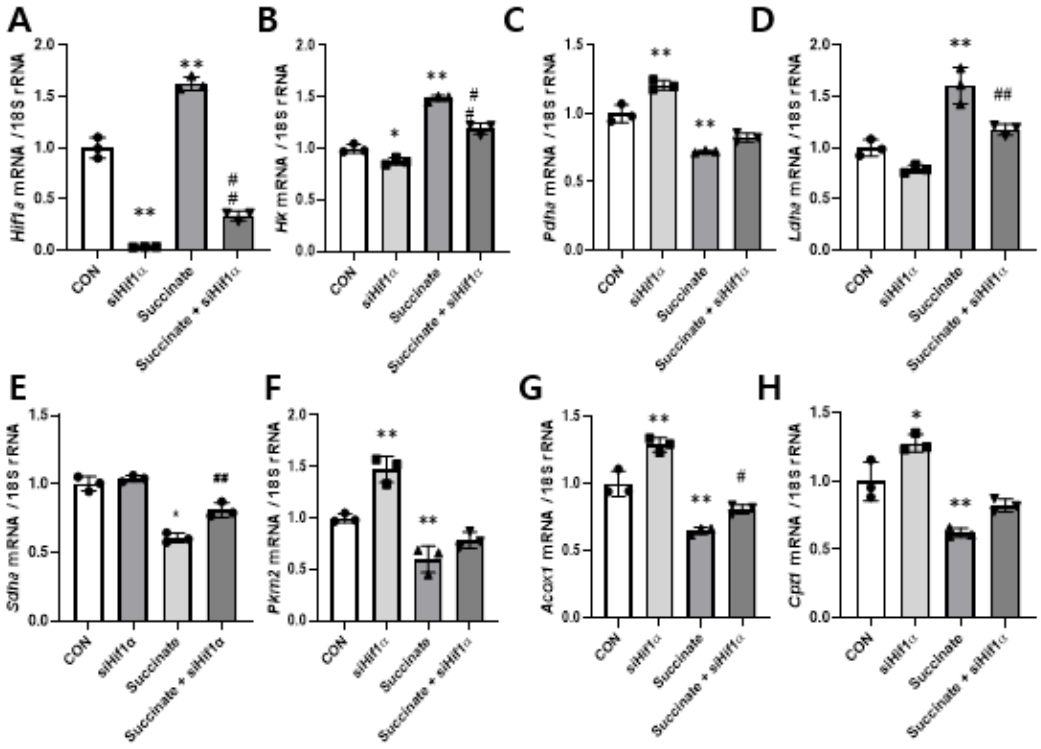

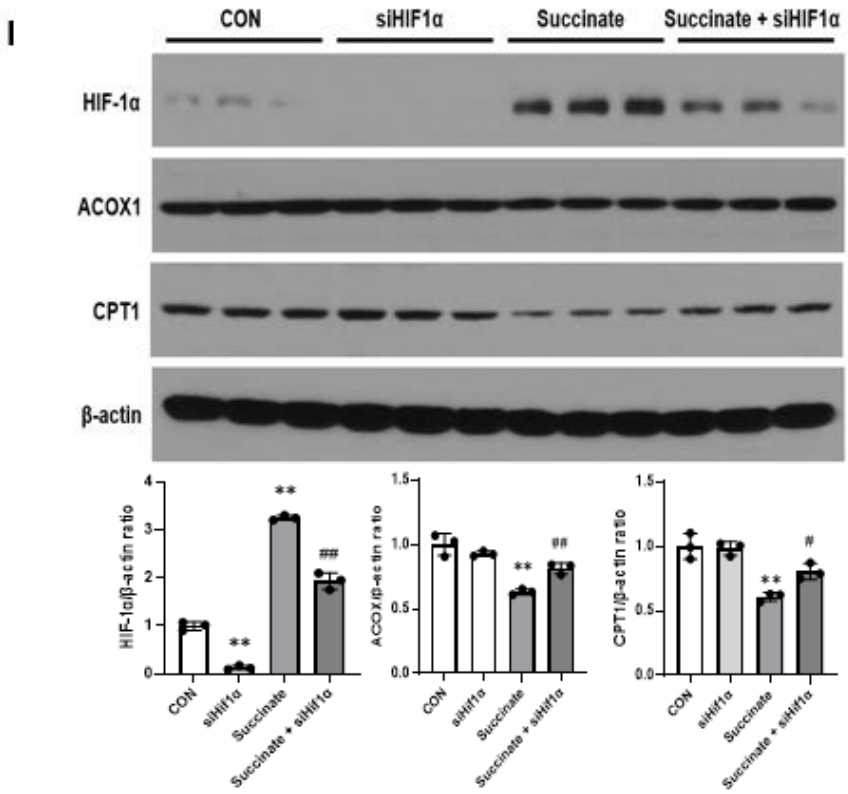

Fig 4. Succinate enhances aberrant glycolysis and suppresses fatty acid oxidation in HG-treated RTECs; Effects reversed by *Hif1a* knockdown.

HG-RTECs were transfected with small interfering RNA (siHIF1α) plasmid or vector plasmid and 40 mM glucose for 48 hours and added with succinate. (A) The *Hif1a* mRNA expression levels were reduced in HG-RTECs transfected with siHIF1α, an effect that was reversed by addition of succinate. (B-D) mRNA expression levels of aberrant glycolysis flux in HG-RTECs transfected with siHIF1α plasmid was reversed by succinate injection (E) mRNA of the succinate dehydrogenase complex flavoprotein subunit A (*Sdha*) is decreased with addition of succinate and increased by siHIF1α. (F) The mRNA level of *Pkm2* were increased in HG-RTECs transfected with siHIF1α which was reversed by succinate addition (G-H) mRNA expression of increased fatty acid oxidation in HG-treated RTECs transfected by siHIF1α plasmid protein was reversed by succinate injection. (I) Protein levels of ACOX1 and CPT1 were reduced with addition of succinate and increased with siHIF1α. HIF1α was increased with succinate addition. Data (n = 3 per group): mean ± standard error of the mean * p <0.05, ** p <0.01 (versus control group (CON)); $^{\#}$ p <0.05, $^{\#\#}$ p <0.01 (versus succinate)

4. PGC-1α directly suppresses HIF-1α transcription via promoter binding in HG-RTECs

Building on the evidence of PGC-1α's indirect regulation of HIF-1α via succinate, I next examined whether PGC-1α could directly regulate HIF-1α transcription. While PGC-1α is a well-established transcriptional coactivator of mitochondrial metabolism-related genes, its role in regulating HIF-1α transcription remains unclear, particularly under diabetic conditions. To test the potential direct interaction between PGC-1α and HIF-1α, ChIP assays were performed with primers spanning the putative hypoxia-responsive element (HRE) region of *Hif1α* promoter. The results showed that *Ppargc1a* binds directly to the *Hif1a* promoter, with significantly increased enrichment in *Ppargc1a*-overexpressing HG-RTECs (Fig 5A-B).

Consistent with the ChIP findings, *Hif1α*-luciferase reporter activity was significantly decreased by *Ppargc1a* overexpression in HG-RTECs (Fig 5C). These results confirm that PGC-1α directly suppresses HIF-1α transcription by binding to its promoter in HG-RTECs. In aggregate, these observations emphasize the direct transcriptional regulatory function of PGC-1α in controlling HIF-1α activity in HG-RTECs.

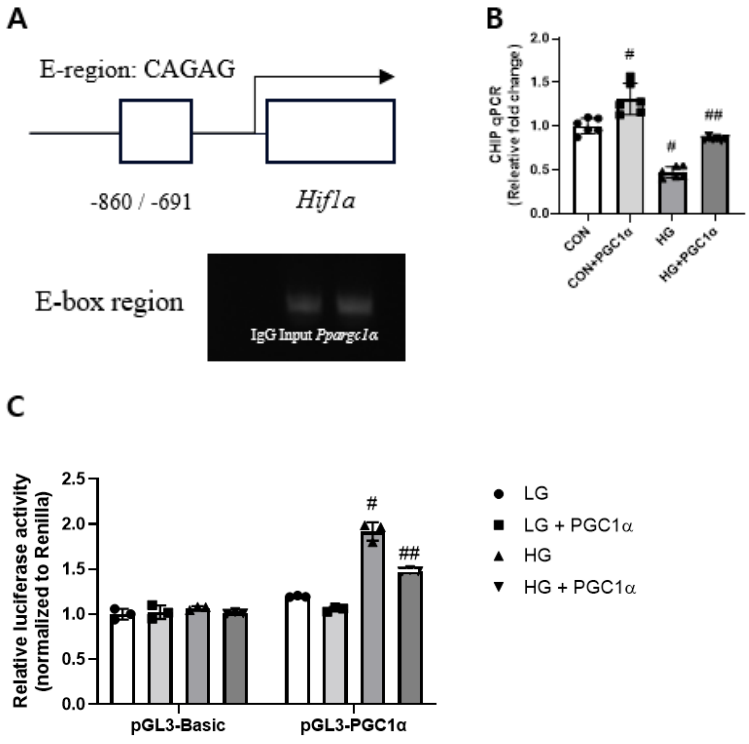

Fig 5. PGC-1α inactivates HIF-1α via direct transcriptional repression in HG-treated RTECs. Primary RTECs were transfected with *Ppargc1a* plasmid (pPGC1α) or small interfering RNA (siPGC1α) plasmid and 40 mM glucose for 48 hours. (A) ChIP assay was performed using a primer that spans the putative hypoxia-responsive element (HRE) region within the E-box flanking region of the *Hif1a* promoter. (B) ChIP-qPCR analysis showed that *Ppargc1a* overexpression significantly increased binding at the *Hif1a* promoter in RTECs under control conditions. This enrichment was reduced under HG conditions and partially restored by *Ppargc1a* overexpression. (C) Luciferase reporter assay in RTECs co-transfected with pGL3-Hif1a and pPGC1α plasmids showed that *Ppargc1a* overexpression significantly suppressed *Hif1a* promoter activity in HG-treated cells. Data (n = 10 per group): mean ± standard error of the mean. $^{\#}$ p <0.01 (versus control group (CON)), $^{\#\#}$ p <0.01 (versus HG)

5. Pharmaceutical activation of PGC-1α activation restores the dysregulated energy metabolism in *db/db* mice

To investigate the potential of PGC-1α activation in mitigating metabolic dysregulation in an *in vivo* diabetic model, I treated *db/db* mice with metformin or resveratrol, both known activators of PGC-1α [24, 25]. Body and kidney weights were recorded in *db/db* and control mice prior to sacrifice. Additionally, biological markers were assessed from the blood and urine samples collected from the mice. The body and kidney mass were increased in *db/db* mice compared to the control group (Table 2). An increase in serum glucose and creatinine levels were observed in *db/db mice* compared to the control group. Metformin and resveratrol treatment influenced the body and kidney weight, serum glucose level, or creatinine level. 24-hour urine albumin excretion at sacrifice was markedly higher in the *db/db* mice compared to the control group, and metformin and resveratrol decreased albuminuria.

Table 2. Body mass, kidney mass, and metabolic parameters

	CON			***db/db***		
	Vehicle	**Metformin**	**Resveratrol**	**Vehicle**	**Metformin**	**Resveratrol**
Body mass (g)	29.2±1.54	30.3±0.88	30.4±1.68	41.3±2.32*	41.3±2.76	40.9±2.5
Kidney mass (g)	0.19±0.02	0.20±0.02	0.20±0.01	0.30±0.01*	0.28±0.01	0.28±0.01
Glucose (mg/dL)	196.2±10.8	214.4±12.4	212.0±15	563.4±68*	536.2±63.8$^{\#}$	563.2±43.2
BUN (mg/dL)	22.2±1.20	21.6±1.60	21.6±1.40	33.4±2.40*	26.8±1.80$^{\#}$	25.8±3.20$^{\#}$
Creatinine (mg/dL)	0.15±0.01	0.14±0.01	0.15±0.02	0.44±0.06*	0.27±0.03$^{\#}$	0.30±0.02$^{\#}$
24-h albuminuria (μg/day)	23.1±2.67	22.4±1.36	23.1±1.98	248.6±24.6*	147.1±5.00$^{\#}$	172.5±16.5$^{\#}$

Data (n = 5 per group): mean ± standard error of the mean
* p <0.05 (versus control group (CON-Vehicle)); $^{\#}$ p <0.05 (versus *db/db*-Vehicle)

Diabetic mice exhibited significantly reduced expression of *Ppargc1a* and *Pkm2*, with a concurrent *Hif1a* level increase compared to controls (Fig 6A-C). Treatment with metformin or resveratrol restored *Ppargc1a* and *Pkm2* expression while reducing *Hif1a* levels. Markers of aberrant glycolysis, including *Glut1, Hk,* and *Ldha,* were elevated in diabetic mice, suggesting increased glycolytic flux and lactate accumulation (Fig 6D-G). Treatment with metformin or resveratrol reversed these metabolic alterations, shifting glucose metabolism away from anaerobic glycolysis. Expression of *Sdha* was lower in *db/db* mice and restored by adding metformin or resveratrol (Fig 6H). Additionally, FAO-related genes *Acox1* and *Cpt1* were downregulated in diabetic mice but significantly restored upon treatment (Fig 6I-J). These findings demonstrate that PGC-1α activation effectively attenuates metabolic inflexibility in *db/db* mice, aligning with my *in vitro* results. The protein level of PGC-1α, HIF-1α, and markers of the FAO exhibited a comparable trend to the mRNA levels with metformin or resveratrol treatment (Fig 6K).

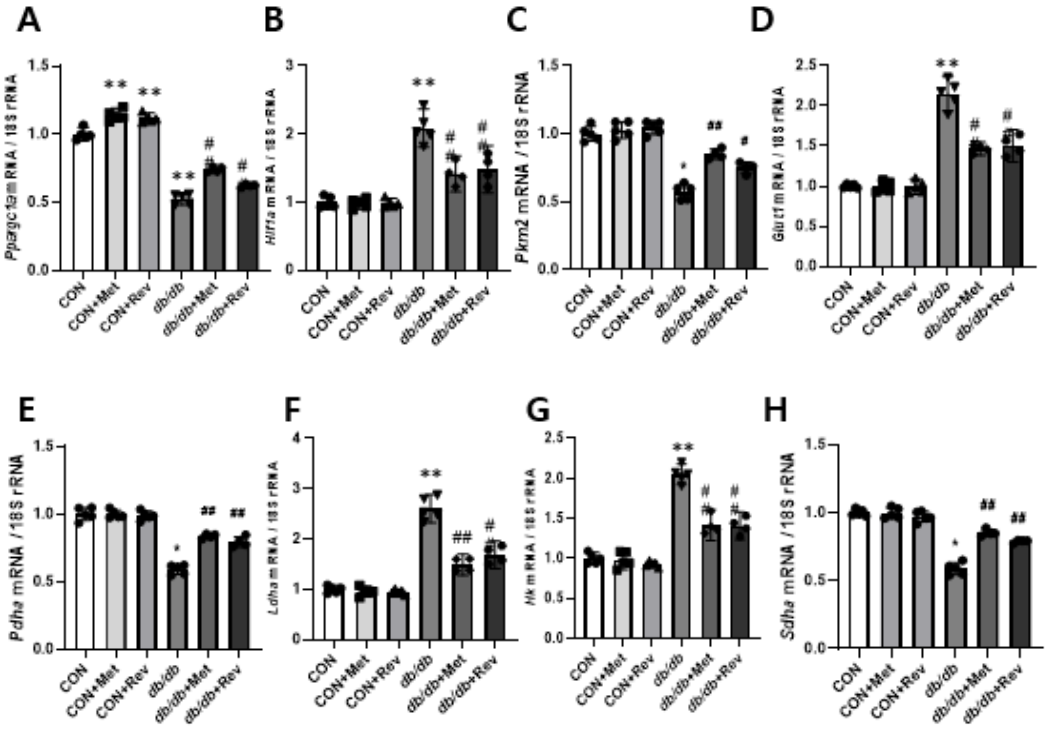

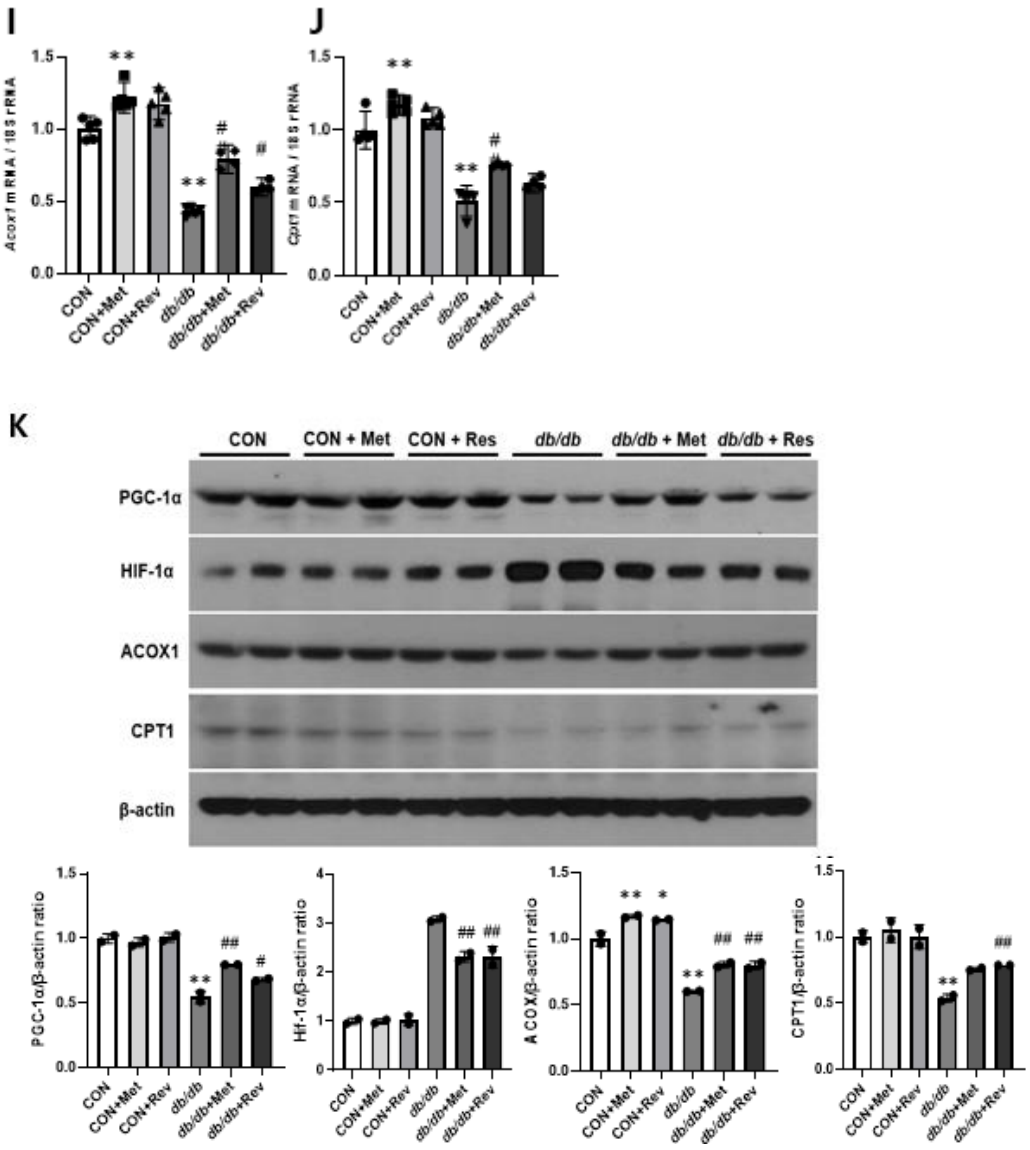

Fig 6. PGC-1α activation by metformin and resveratrol restores metabolic balance in *db/db* mice. Both *db/db* and control mice were given metformin (200 mg/kg/day) and resveratrol (20mg/kg/day) via gavage for 12 weeks. (A) *Ppargc1a* mRNA expression levels were decreased in *db/db* mice; however, this reduction was reversed by treatment with metformin and resveratrol. (B) The mRNA level of *Hif1a* was higher in *db/db* mice, which were decreased by metformin and resveratrol. (C) The mRNA expression level of *Pkm2* decreased in *db/db* mice and enhanced by metformin and resveratrol. (D-G) The mRNA levels of glycolysis pathway were altered in *db/db* mice, those which were restored by metformin and resveratrol. (H) The mRNA expression level of *Sdha* was decreased in *db/db* mice, which was reversed by metformin and resveratrol. (I-J) The

mRNA expression levels of *Cpt1* and *Acox1*, were reduced in *db/db* mice and these were increased by metformin and resveratrol. (K) PGC-1α, ACOX1, and CPT1 protein expressions were reduced in *db/db* mice, and increased by metformin or resveratrol. HIF-1α was increased in *db/db* mice, while decreased by metformin or resveratrol. Data (n = 5 per group): mean ± standard error of the mean * p <0.05, ** p <0.01 (versus control group (CON)); $^{\#}$ p <0.05, $^{\#\#}$ p <0.01 (versus *db/db*)

6. PGC-1α activation attenuates altered mitochondrial dynamics, structure, and activity in HG-RTECs and *db/db* mice

Lastly, I examined mitochondrial dynamics, structure, and activity in HG-RTECs and *db/db* mice. In HG-RTECs, *Mfn1*, a mitochondrial outer membrane fusion-related gene was decreased. In contrast, *Drp1*, a mitochondrial fission-related gene, was elevated in HG-RTECs. Overexpression of *Ppargc1a* reversed the mRNA of these genes and the corresponding protein levels (Fig 7A-C). Silencing of *Ppargc1a* decreased the mRNA levels of *Mfn1* and increased those of *Drp1*, as well as the subsequent protein levels (Fig 7D-F). Similarly, in *db/db* mice, the *Mfn1* mRNA expression was substantially decreased, while *Drp1*, a mitochondrial fission-related gene, was raised (Fig 7G-H). Metformin and resveratrol treatment restored these changes. Oxidative stress levels were measured by MitoSox staining (Fig 7I). Mitochondria-generated ROS were increased in HG-RTECs in comparison to the control group. The observed increase was diminished by overexpression of *Ppargc1a* or silencing by siHIFα. Conversely, this change was increased by silencing *Ppargc1a* with siPGC1α or addition of succinate. Electron microscopy also showed fragmented mitochondria and disrupted cristae in RTECs of diabetic kidney, and these abnormalities were significantly improved by metformin or resveratrol (Fig 7J).

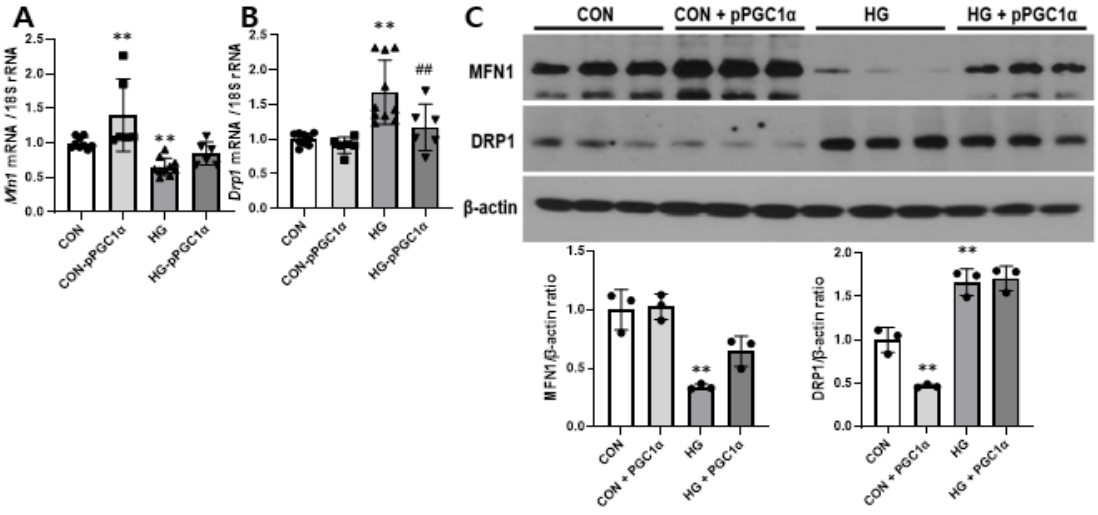

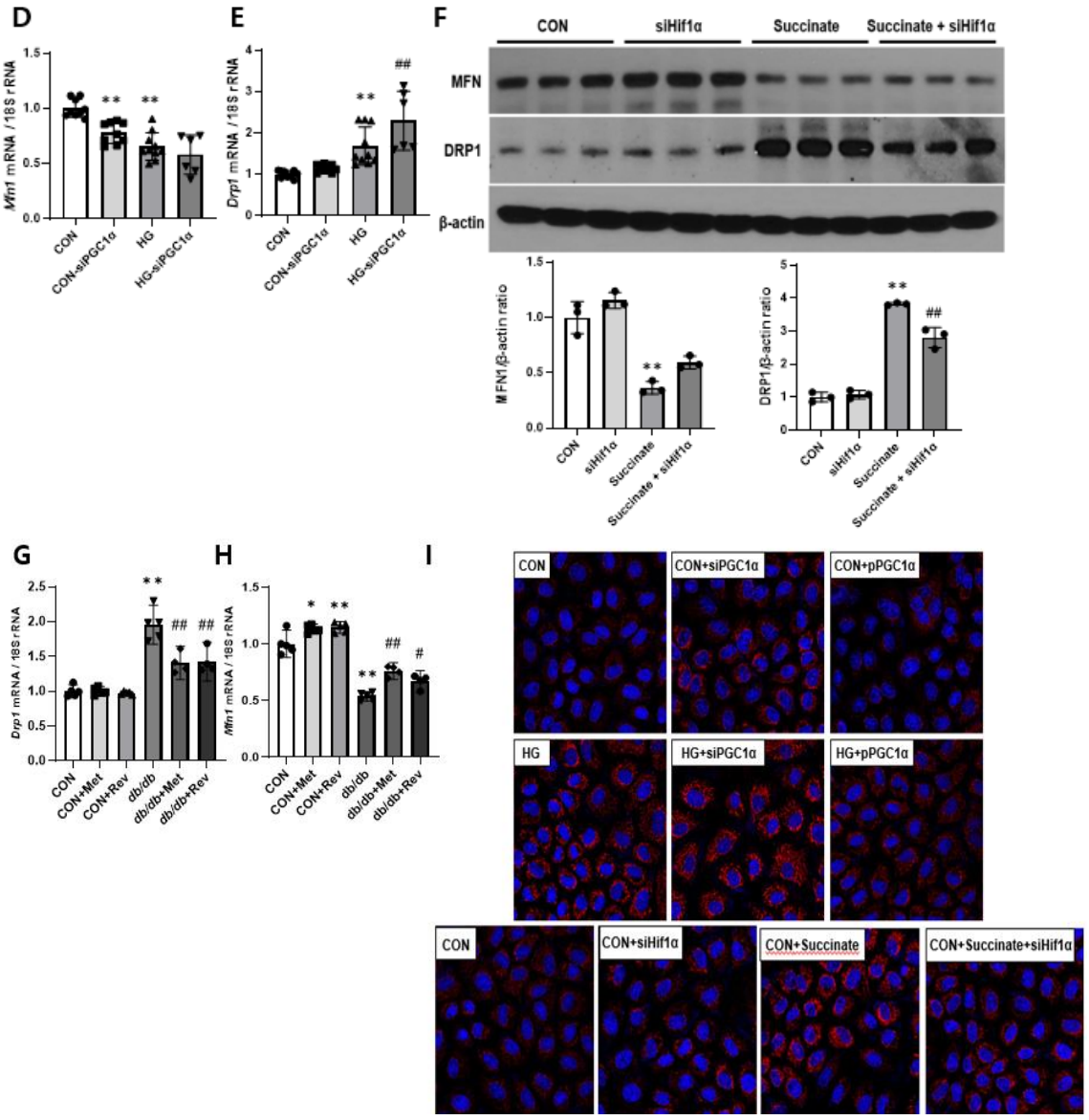

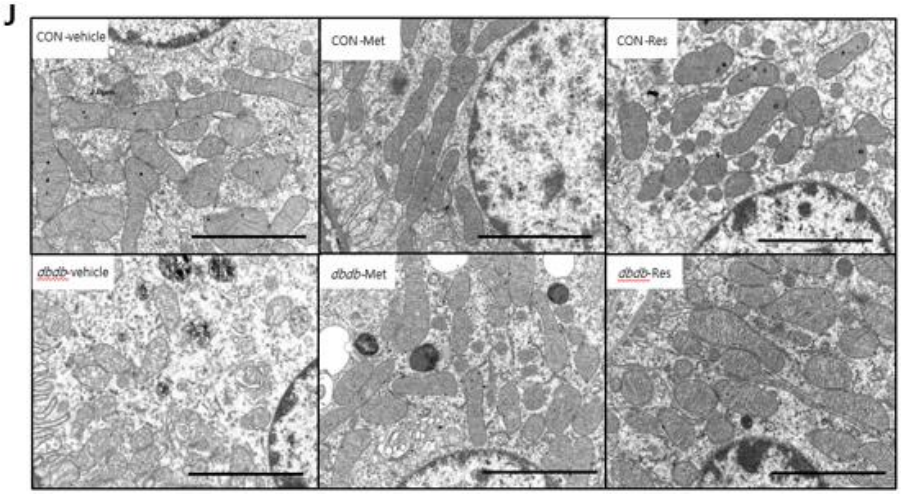

Fig 7. PGC-1α activation via metformin and resveratrol restores altered mitochondrial dynamics and structure in HG-RTECs and *db/db* mice. Primary RTECs were stimulated with 40 mM glucose (HG) and transfected with *Ppargc1a* plasmid (pPGC1α) or vector plasmid and 40 mM glucose for 48 hours. (A-B) The expression of *Mfn1* and *Drp1* mRNA showed a shift toward mitochondrial fragmentation in HG-RTECs. (C) protein level of MFN1 was reduced in HG-RTECs and reversed by *Ppargc1a* overexpression. DRP1 was increased in HG-RTECs and reversed by *Ppargc1a* overexpression. (D-F) Silencing with small interfering RNA (siPGC1α) plasmid showed opposite results. (G-H) In *db/db* mice, the mRNA levels of *Mfn* and *Drp1* exhibited a change in mitochondrial dynamics toward fission. These alterations were attenuated by metformin or resveratrol administration. (I) Confocal microscopy analysis using MitoSOX staining demonstrated increased mitochondria-derived ROS in HG-RTECs. This increase was attenuated by overexpression of *Ppargc1a* or siHIF1α, and elevated by silencing *Ppargc1a* or adding succinate. (J) Electron microscopy of *db/db* mice showed increased mitochondrial fission and structural disruption of kidney mitochondria of *db/db* mice compared to the control group. Metformin or resveratrol attenuated this change. (scale bar = 2000 nm). Data (n = 5 per group): mean ± standard error of the mean ** p <0.01 (versus control group (CON)); $^{\#\#}$ p <0.01 (versus *db/db* or HG group or succinate group)

7. PGC-1α activation attenuates apoptosis and profibrotic markers in HG-RTECs

The aberrant energy metabolism and mitochondrial injury in DKD leads to apoptosis and kidney fibrosis. The mRNA and protein expression levels of profibrotic-and apoptosis-related markers increased in HG-RTECs. An increase in mRNA and protein expression of fibrotic- and apoptosis related markers was observed in HG-RTECs. Overexpression of *Ppargc1a* resulted in reduction of these markers. (Fig 8A-D). Silencing of *Ppargc1a* resulted in an increase of these markers (Fig 8E-H). Addition of succinate resulted in an increase of these markers, however silencing *Hif1a* decreased them (Fig 8I-L).

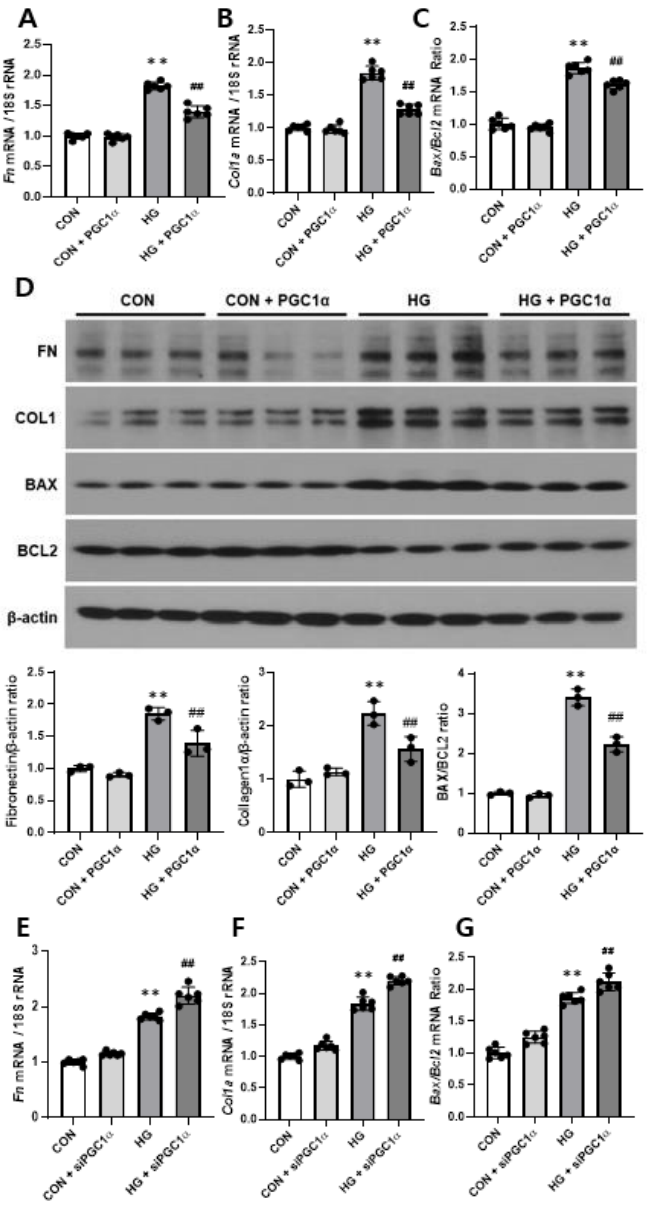

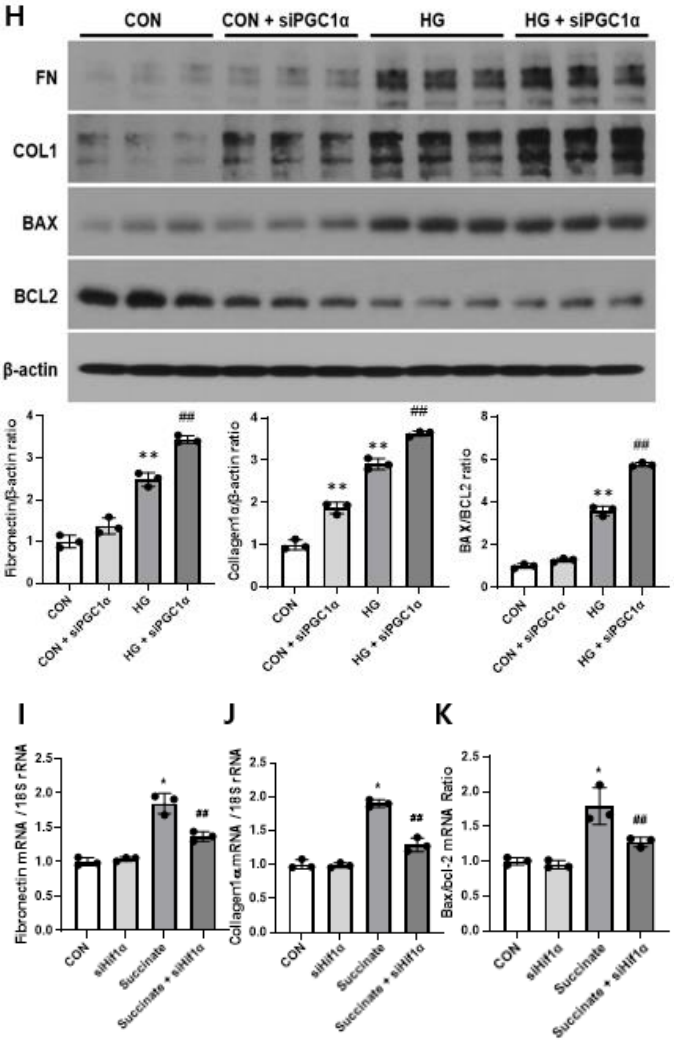

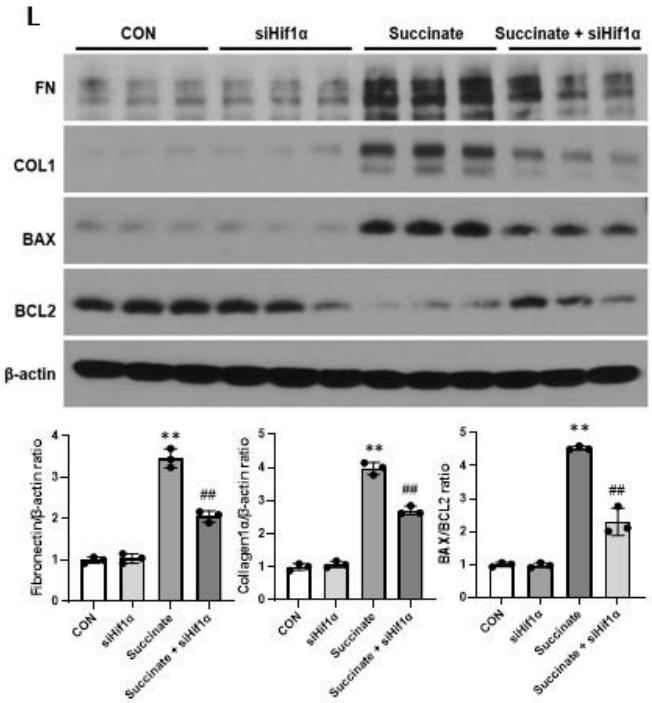

Fig 8. PGC-1α activation decreases apoptosis and profibrotic markers in HG-RTECs.
For 48 hours, primary RTECs were stimulated with 40 mM glucose (HG) and transduced with either the *Ppargc1a* plasmid (pPGC1α) or control vector plasmid. (A-D) The mRNA and protein levels of apoptotic cell death markers and fibrosis associated makers were increased in HG-RTECs compared with control group. Addition of pPGC1α plasmid attenuated this change. (E-H) Addition of siPGC1α plasmid aggravated this change. (I-L) Addition of succinate aggravated apoptosis and fibrosis related markers and addition of siHIF1α plasmid attenuated these markers. Data (n = 10 per group): mean ± standard error of the mean * p <0.05 (*versus* control group (CON)); $^{\#\#}$ p <0.01 (versus HG or succinate group)

In *db/db* mice, the fibrotic- and apoptosis-related markers was increased, and the addition of metformin or resveratrol attenuated these increases (Fig 9).

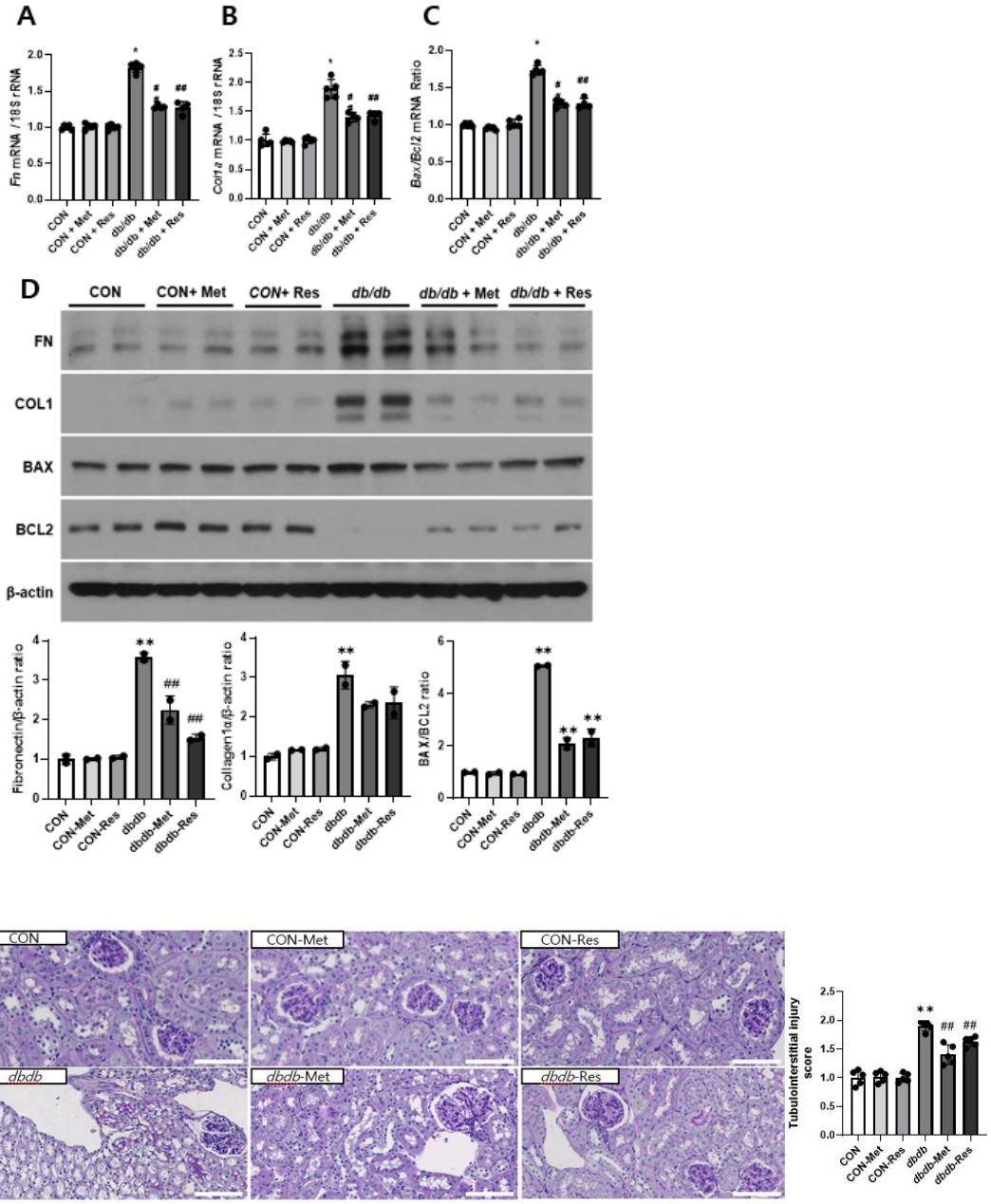

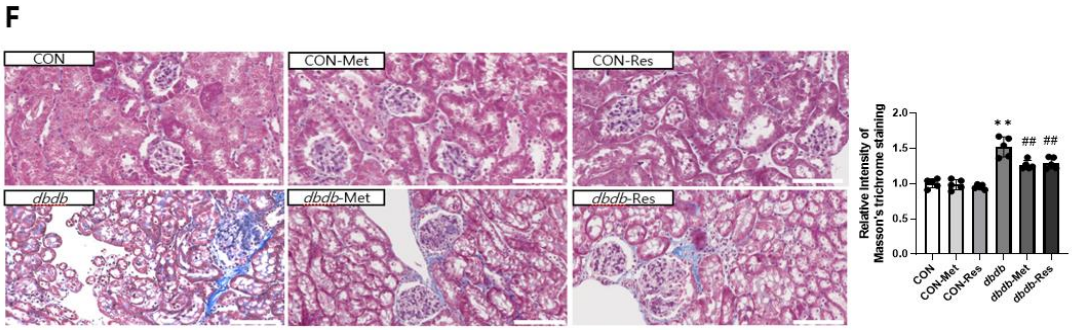

Fig 9. PGC-1α activation via metformin and resveratrol treatment reduces renal fibrotic changes in *db/db* mice. (A-D) Both mRNA and protein levels of apoptosis- and fibrosis-related markers were upregulated in *db/db* mice compared to the control group. Administration of metformin and resveratrol attenuated this change. Transfection with siPGC1α plasmid aggravated this change, and addition of pPGC1α plasmid attenuated this change. Renal fibrosis was reduced in *db/db* mice treated with metformin and resveratrol, as shown by (E) PAS and (F) Masson's trichrome staining. Data (n = 5 per group): mean ± standard error of the mean Scale bar = 100 μm. * p <0.05, ** p <0.01 (versus control group (CON)); $^{\#\#}$ p <0.05, $^{\#\#}$ p <0.01 (versus *db/db*)

4. DISCUSSION

This study was designed to investigate the relationship between PGC-1α and HIF-1α in the context of DKD. I demonstrated that HG-treated RTECs and diabetic mice exhibit a coordinated pattern of metabolic dysregulation, characterized by reduced PGC-1α and PKM2 expression, elevated HIF-1α levels, increased aberrant glycolytic flux, impaired FAO, and decreased TCA cycle enzyme activity. Overexpression of PGC-1α reversed these metabolic disturbances, whereas PGC-1α silencing further aggravated them. Conversely, silencing HIF-1α led to increased PGC-1α and PKM2 expression, suppression of glycolytic reprogramming, restoration of FAO, and reactivation of the TCA cycle, which were counteracted by succinate treatment. Notably, PGC-1α directly suppressed HIF-1α transcription by binding to its HIF-1α promoter region, and this interaction was attenuated by elevated succinate, a TCA intermediate that inhibits HIF-1α degradation. The proposed model highlights how PGC-1α integrates transcriptional and metabolic cues to suppress HIF-1α activity and restore mitochondrial energy homeostasis under diabetic conditions (Fig 10).

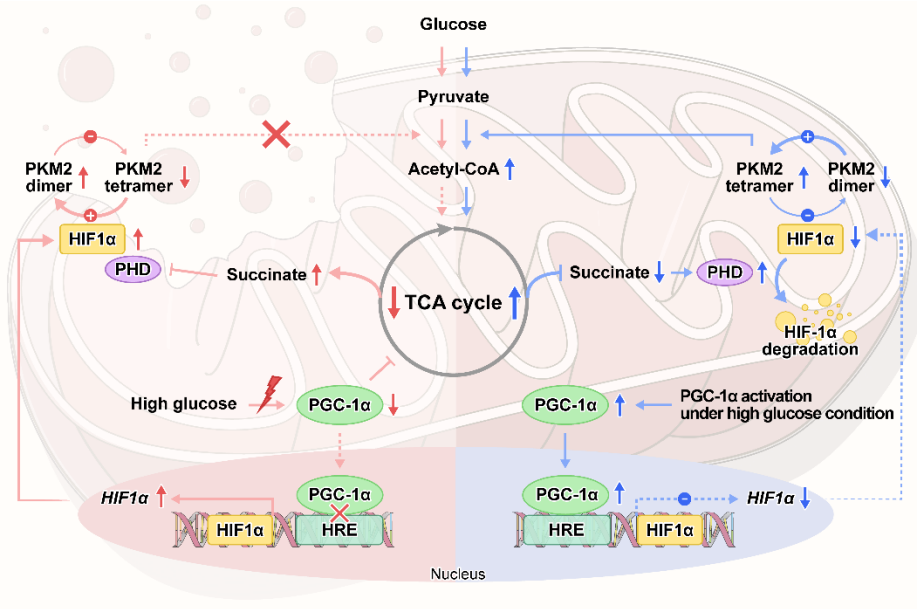

Fig 10. Graphical summary
Under high glucose conditions, PGC-1α inactivation induces TCA cycle dysfunction and succinate elevation, which leads to increased HIF-1α levels and decreased PKM2 activity. Additionally, PGC-1α inactivation reduces the binding of PGC-1α to the HIF-1α promoter, resulting in increased HIF-1α transcription.

Previous studies have shown that early-stage DKD has increased aerobic glycolysis and FAO, leading to enhanced ATP production [15, 45]. However, in late stage DKD involves a metabolic shift toward anaerobic glycolysis and suppressed FAO, resulting in impaired TCA cycle activity and reduced ATP production [46, 47]. This transition has been attributed to the accumulation of toxic intermediates from the TCA cycle and glycolysis [48, 49]. In line with these findings, my study confirmed that the HG-RTECs and *db/db* mice exhibited increased anaerobic glycolysis, decreased FAO, suppressed TCA cycle activity, and elevated levels of TCA cycle intermediates compared to the controls – features characteristics of late-stage DKD. While these observations are consistent with prior reports, a deeper understanding of DKD progression requires investigating the interplay among key regulatory factors. My study focused on the roles of PGC-1α. HIF-1α, and the TCA cycle intermediate succinate as key regulators of metabolic dysfunction in DKD.

A large body of evidence have demonstrated that hyperglycemia lowered both the expression and activity of PGC-1α [50-52]. This reduction has also been observed in DKD, where decreased PGC-1α levels are reported in podocytes and RTECS under hyperglycemic conditions [53, 54]. As a principal modulator of mitochondrial biogenesis, decreased PGC-1α contributes to enhanced aberrant glycolysis, impaired FAO, and mitochondrial dysfunction leading to cell apoptosis and kidney fibrosis. I reconfirm these associations, as *Ppargc1a* expression was decreased in *db/db* mice

and HG-RTECs, alongside increased *Glut1*, *Hk*, *Ldha*, and reduced *Sdha* expression. Notably, restoring PGC-1α reversed these alterations in both HG-RTECs and *db/db* mice. Given that PGC-1α modulates multiple downstream factors, further exploration of these regulators may offer therapeutic potential for kidney function preservation [55].

Prior research has suggested that the reduction of PGC-1α impairs in TCA cycle activity, leading to the accumulation of intermediates such as succinate [56, 57]. Elevated succinate inhibits PHD, thereby stabilizing HIF-1α [58], positioning succinate as another metabolic regulator of HIF-1α activity in DKD. In my study, succinate levels were elevated in HG-RTECs, and further increased with *Ppargc1a* silencing, while *Ppargc1a* overexpression reduced succinate accumulation. Functionally, succinate administration increased *Hif1a* levels and suppressed *Pkm2*, accompanied by enhanced aberrant glycolysis, decreased TCA cycle enzyme activity, and reduced FAO. These metabolic alterations were partially reversed by simultaneous *Hif1a* silencing, which restored *Pkm2* levels, reduced aberrant glycolysis, and improved FAO. Together, these results support a model in which PGC-1α deficiency promotes succinate accumulation, leading to HIF-1α stabilization and downstream metabolic dysfunction in DKD.

HIF-1α, a key modulator of the cellular response to glycolysis and hypoxia, plays an important role in DKD progression. While previous studies have shown that HIF-1α may exert a protective effect during early DKD, its sustained activation in later stages contributes to kidney function decline and fibrosis [59, 60]. HIF-1α is known to upregulate glucose transporters such as GLUT1 and GLUT3, also enhance anaerobic glycolysis through activation of enzymes including HK1, HK2, phosphoglycerate kinase1, PKM2, and LDHA [36]. Consistent with its established role, my study highlights HIF-1α as a central metabolic regulator. Notably, silencing HIF-1α in HG-treated RTECs led to increased *Pkm2* expression, reduced aberrant glycolysis, improved FAO, and reactivation of the TCA cycle activity, reinforcing the pathological role of sustained HIF-1α activation in DKD.

A growing body of evidence has suggested a significant relationship between PGC-1α and HIF-1α. However, no study to date has clearly defined the direct interplay between these two regulators in the context of DKD. Interestingly, emerging data point to a collaborative network involving PGC-1α, HIF-1α, and PKM2. Several studies have reported an inhibitory effect of HIF-1α on PGC-1α activity in DKD, as well as in renal cancer cells and hepatocytes [39, 40]. In addition, Qi et al. demonstrated that pharmacologic activation of PKM2 with TEPP-46 preserved PGC-1α function and reversed altered mitochondrial metabolism in the podocytes of DKD [42]. Our group further elucidated the mechanistic link between PKM2 and PGC-1α, showing that HIF-1α directly regulates PGC-1α in a PKM2 dependent manner [43]. Complementing this, Palsson-McDermott et al. showed that PKM2 activation by either TEPP-46 or DASA-58 inhibited LPS-induced HIF-1α expression [26]. Building on these insights, this study was initiated with the hypothesis that a mutual regulatory relationship exists between PGC-1α and HIF-1α under hyperglycemic conditions. Based on my results, I clearly showed that hyperglycemia-driven PGC-1α deficiency leads to decreased

TCA cycle activity and succinate accumulation, resulting in enhanced HIF-1α activity. Moreover, using ChIP and luciferase reporter assays, I demonstrated that PGC-1α directly binds to the HRE within the *Hif1a* promoter of HG-RTECs, thereby suppressing its transcription. Overexpression of *Ppargc1a* in HG-RTECs using *Ppargc1a* plasmid significantly increased the abundance of HRE-binding region in the *Hif1a* promoter and reduced HIF-1α expression. These findings reveal direct inhibitory interaction between PGC-1α and HIF-1α in HG-RTECs.

There are several limitations to this study. First, I used metformin and resveratrol as pharmacologic activators of PGC-1α. Although both agents are known to stimulate PGC-1α, they also have additional effects beyond PGC-1α activation. For instance, metformin lowers glucose levels by enhancing insulin sensitivity and increasing glucose uptake in muscle tissue, which may confer indirect renal benefits. However, in this study, metformin reduced blood glucose levels by only 10%, suggesting that its glucose-lowering effect alone may not fully account for the observed reno-protective effects, while its broader metabolic benefits likely remain relevant. Resveratrol, though less potent, also possesses antioxidant, anti-inflammatory properties, and improves insulin sensitivity-factors that can influence metabolic outcomes independent of PGC-1α. To more specifically evaluate the role of PGC-1α, future studies should consider using direct PGC-1α activators, which would allow for more targeted mechanistic exploration. Second, I did not use knock out mouse models to validate the *in vitro* study. While I manipulated *Ppargc1a* on and *Hif1a* expression through overexpression and silencing in cultured RTECs, the use of genetically modified mouse models would have provided stronger causal evidence for their roles in DKD pathogenesis.

5. CONCLUSION

In this study, I demonstrated that PGC-1α plays a dual regulatory role in modulating HIF-1α activity under diabetic conditions. Specifically, reduced PGC-1α expression in high-glucose environments led to the accumulation of TCA cycle intermediates, particularly succinate, which in turn stabilized HIF-1α and contributed to mitochondrial metabolic dysfunction. In addition to this indirect mechanism, PGC-1α was shown to directly suppress HIF-1α transcription through promoter binding, a process attenuated by elevated succinate levels. These findings offer mechanistic insight into how impaired PGC-1α signaling under diabetic conditions disrupts mitochondrial energy homeostasis, highlighting its relevance in the pathogenesis of diabetic kidney disease.

REFERENCES

1 K. L. Johansen *et al.*, "US Renal Data System 2023 annual data report: Epidemiology of kidney disease in the United States," *Am. J. Kidney. Dis.,* vol. 83, no. 4, pp. A8–A13, 2024.

2 U. S. Renal Data System, "2018 USRDS annual data report: Epidemiology of kidney disease in the United States," 2018. [Online]. Available: https*://www. usrds. org/adr. aspx*

3 Z. Wang *et al.*, "Specific metabolic rates of major organs and tissues across adulthood: evaluation by mechanistic model of resting energy expenditure," *Am. J. Clin. Nutr.,* vol. 92, no. 6, pp. 1369–1377, 2010.

4 P. M. O'Connor, "Renal oxygen delivery: matching delivery to metabolic demand," *Clin. Exp. Pharmacol. Physiol.,* vol. 33, no. 10, pp. 961–967, 2006.

5 G. Wirthensohn and W. G. Guder, "Renal substrate metabolism," *Physiol. Rev.,* vol. 66, no. 2, pp. 469–497, 1986.

6 J. H. Thaysen, N. Lassen, and O. Munck, "Sodium transport and oxygen consumption in the mammalian kidney," *Nature,* vol. 190, no. 4779, pp. 919–921, 1961.

7 L. Mandel and R. Balaban, "Stoichiometry and coupling of active transport to oxidative metabolism in epithelial tissues," *Am. J. Physiol.,* vol. 240, no. 5, pp. F357–F371, 1981.

8 D. J. Pagliarini *et al.*, "A mitochondrial protein compendium elucidates complex I disease biology," *Cell,* vol. 134, no. 1, pp. 112–123, 2008.

9 J. M. Forbes and D. R. Thorburn, "Mitochondrial dysfunction in diabetic kidney disease," *Nat. Rev. Nephrol.,* vol. 14, no. 5, pp. 291–312, 2018.

10 H. Qi *et al.*, "Glomerular endothelial mitochondrial dysfunction is essential and characteristic of diabetic kidney disease susceptibility," *Diabetes,* vol. 66, no. 3, pp. 763–778, 2017.

11 W. Qi *et al.*, "Pyruvate kinase M2 activation may protect against the progression of diabetic glomerular pathology and mitochondrial dysfunction," *Nat. Med.,* vol. 23, no. 6, pp. 753–762, 2017.

12 Y. Chen, B. C. Fry, and A. T. Layton, "Modeling glucose metabolism and lactate production in the kidney," *Math. Biosci.,* vol. 289, pp. 116–129, 2017.

13 C. Scott, "Misconceptions about aerobic and anaerobic energy expenditure," *J. Int. Soc. Sports Nutr.,* vol. 2, no. 2, p. 32, 2005.

14 O. Warburg, "On the origin of cancer cells," *Science,* vol. 123, no. 3191, pp. 309–314, 1956.

15 K. M. Sas *et al.*, "Tissue-specific metabolic reprogramming drives nutrient flux in diabetic complications," *JCI insight,* vol. 1, no. 15, 2016.

16 K. Sharma *et al.*, "Metabolomics reveals signature of mitochondrial dysfunction in diabetic kidney disease," (in eng), *J. Am. Soc. Nephrol.,* vol. 24, no. 11, pp. 1901–12, Nov. 2013, doi: 10.1681/asn.2013020126.

17 M. G. Vander Heiden, L. C. Cantley, and C. B. Thompson, "Understanding the Warburg effect: the metabolic requirements of cell proliferation," *Science,* vol. 324, no. 5930, pp. 1029–1033, 2009.

18 S. Kierans and C. Taylor, "Regulation of glycolysis by the hypoxia-inducible factor (HIF):

implications for cellular physiology," *J. Physiol.,* vol. 599, no. 1, pp. 23–37, 2021.

19 Z. Arany *et al.*, "Transcriptional coactivator PGC-1α controls the energy state and contractile function of cardiac muscle," *Cell Metab.,* vol. 1, no. 4, pp. 259–271, 2005.

20 Z. Wu *et al.*, "Mechanisms controlling mitochondrial biogenesis and respiration through the thermogenic coactivator PGC-1," *Cell,* vol. 98, no. 1, pp. 115–124, 1999.

21 C. Handschin and B. M. Spiegelman, "Peroxisome proliferator-activated receptor γ coactivator 1 coactivators, energy homeostasis, and metabolism," *Endocr. Rev.,* vol. 27, no. 7, pp. 728–735, 2006.

22 K. Guo *et al.*, "Protective role of PGC-1α in diabetic nephropathy is associated with the inhibition of ROS through mitochondrial dynamic remodeling," *PLoS ONE,* vol. 10, no. 4, p. e0125176, 2015.

23 L. Zhang, J. Liu, F. Zhou, W. Wang, and N. Chen, "PGC-1α ameliorates kidney fibrosis in mice with diabetic kidney disease through an antioxidative mechanism," *Mol. Med. Rep.,* vol. 17, no. 3, pp. 4490–4498, 2018.

24 M. Lagouge *et al.*, "Resveratrol improves mitochondrial function and protects against metabolic disease by activating SIRT1 and PGC-1α," *Cell,* vol. 127, no. 6, pp. 1109–1122, 2006.

25 M. Suwa, T. Egashira, H. Nakano, H. Sasaki, and S. Kumagai, "Metformin increases the PGC-1α protein and oxidative enzyme activities possibly via AMPK phosphorylation in skeletal muscle in vivo," *J. Appl. Physiol.,* vol. 101, no. 6, pp. 1685–1692, 2006.

26 E. M. Palsson-McDermott *et al.*, "Pyruvate kinase M2 regulates Hif-1α activity and IL-1β induction and is a critical determinant of the warburg effect in LPS-activated macrophages," *Cell Metab.,* vol. 21, no. 1, pp. 65–80, 2015.

27 C. Chen, N. Pore, A. Behrooz, F. Ismail-Beigi, and A. Maity, "Regulation of glut1 mRNA by hypoxia-inducible factor-1: interaction between H-ras and hypoxia," *J. Biol. Chem.,* vol. 276, no. 12, pp. 9519–9525, 2001.

28 V. Infantino, A. Santarsiero, P. Convertini, S. Todisco, and V. Iacobazzi, "Cancer cell metabolism in hypoxia: Role of HIF-1 as key regulator and therapeutic target," *Int. J. Mol. Sci.,* vol. 22, no. 11, p. 5703, 2021.

29 M. S. Nakazawa, B. Keith, and M. C. Simon, "Oxygen availability and metabolic adaptations," *Nat. Rev. Cancer,* vol. 16, no. 10, pp. 663–673, 2016.

30 H. Xie and M. C. Simon, "Oxygen availability and metabolic reprogramming in cancer," *J. Biol. Chem.,* vol. 292, no. 41, pp. 16825–16832, 2017.

31 P. Maxwell *et al.*, "Hypoxia-inducible factor-1 modulates gene expression in solid tumors and influences both angiogenesis and tumor growth," *Proc. Natl. Acad. Sci. U.S.A,* vol. 94, no. 15, pp. 8104–8109, 1997.

32 W. Luo *et al.*, "Pyruvate kinase M2 is a PHD3-stimulated coactivator for hypoxia-inducible factor 1," *Cell,* vol. 145, no. 5, pp. 732–744, 2011.

33 J.-W. Kim, P. Gao, Y.-C. Liu, G. L. Semenza, and C. V. Dang, "Hypoxia-inducible factor 1 and dysregulated c-Myc cooperatively induce vascular endothelial growth factor and metabolic switches hexokinase 2 and pyruvate dehydrogenase kinase 1," *Mol. Cell. Biol.,*

vol. 27, no. 21, pp. 7381–7393, 2007.

34 G. Qing *et al.*, "Combinatorial Regulation of Neuroblastoma Tumor Progression by N-Myc and Hypoxia Inducible Factor HIF-1αN-Myc and HIF-1α in Neuroblastoma," *Cancer Res.,* vol. 70, no. 24, pp. 10351–10361, 2010.

35 W. W. Wheaton and N. S. Chandel, "Hypoxia. 2. Hypoxia regulates cellular metabolism," *Am. J. Physiol. Cell Physiol.,* vol. 300, no. 3, pp. C385–C393, 2011.

36 J.-W. Kim, I. Tchernyshyov, G. L. Semenza, and C. V. Dang, "HIF-1-mediated expression of pyruvate dehydrogenase kinase: a metabolic switch required for cellular adaptation to hypoxia," *Cell Metab.,* vol. 3, no. 3, pp. 177–185, 2006.

37 I. Papandreou, R. A. Cairns, L. Fontana, A. L. Lim, and N. C. Denko, "HIF-1 mediates adaptation to hypoxia by actively downregulating mitochondrial oxygen consumption," *Cell Metab.,* vol. 3, no. 3, pp. 187–197, 2006.

38 A. Morin, E. Letouzé, A. P. Gimenez-Roqueplo, and J. Favier, "Oncometabolites-driven tumorigenesis: from genetics to targeted therapy," *Int. J. Cancer,* vol. 135, no. 10, pp. 2237–2248, 2014.

39 Y. Liu *et al.*, "HIF-1α and HIF-2α are critically involved in hypoxia-induced lipid accumulation in hepatocytes through reducing PGC-1α-mediated fatty acid β-oxidation," *Toxicol. Lett.,* vol. 226, no. 2, pp. 117–123, 2014.

40 K. Tsukada *et al.*, "Hypoxia-inducible factor-1 is a determinant of lobular structure and oxygen consumption in the liver," *Microcirculation,* vol. 20, no. 5, pp. 385–393, 2013.

41 E. L. LaGory *et al.*, "Suppression of PGC-1α is critical for reprogramming oxidative metabolism in renal cell carcinoma," *Cell Rep.,* vol. 12, no. 1, pp. 116–127, 2015.

42 W. Qi *et al.*, "Pyruvate kinase M2 activation may protect against the progression of diabetic glomerular pathology and mitochondrial dysfunction," *Nat. Med.,* vol. 23, no. 6, pp. 753–762, 2017.

43 Y. S. Joo, "Pharmacologic pyruvate kinase M2 activation maintains mitochondrial metabolism by regulating the interaction between HIF-1α and PGC-1α in diabetic kidney disease," Ph.D dissertation, Depart. of Medicine, The Graduate School, Yonsei Univ., 2023.

44 G. Sun, M. A. Reddy, H. Yuan, L. Lanting, M. Kato, and R. Natarajan, "Epigenetic Histone Methylation Modulates Fibrotic Gene Expression," *J. Am. Soc. Nephrol.,* vol. 21, no. 12, pp. 2069–2080, 2010, doi: 10.1681/asn.2010060633.

45 M. Li *et al.*, "GC/TOFMS analysis of metabolites in serum and urine reveals metabolic perturbation of TCA cycle in db/db mice involved in diabetic nephropathy," *Am. J. Physiol-Renal Physiol.,* vol. 304, no. 11, pp. F1317–F1324, 2013.

46 P. Dhillon *et al.*, "The nuclear receptor ESRRA protects from kidney disease by coupling metabolism and differentiation," *Cell Metab.,* vol. 33, no. 2, pp. 379–394. e8, 2021.

47 H. M. Kang *et al.*, "Defective fatty acid oxidation in renal tubular epithelial cells has a key role in kidney fibrosis development," *Nat. Med.,* vol. 21, no. 1, pp. 37–46, 2015.

48 W. He *et al.*, "Citric acid cycle intermediates as ligands for orphan G-protein-coupled receptors," *Nature,* vol. 429, no. 6988, pp. 188–193, 2004.

49 I. Toma *et al.*, "Succinate receptor GPR91 provides a direct link between high glucose

levels and renin release in murine and rabbit kidney," *J. Clin. Invest.,* vol. 118, no. 7, pp. 2526–2534, 2008.

50 K. Hara *et al.*, "A genetic variation in the PGC-1 gene could confer insulin resistance and susceptibility to Type II diabetes," *Diabetologia,* vol. 45, pp. 740–743, 2002.

51 Y. L. Muller, C. Bogardus, O. Pedersen, and L. Baier, "A Gly482Ser missense mutation in the peroxisome proliferator-activated receptor γ coactivator-1 is associated with altered lipid oxidation and early insulin secretion in Pima Indians," *Diabetes,* vol. 52, no. 3, pp. 895–898, 2003.

52 V. K. Mootha *et al.*, "PGC-1α-responsive genes involved in oxidative phosphorylation are coordinately downregulated in human diabetes," *Nat. Genet.,* vol. 34, no. 3, pp. 267–273, 2003.

53 H. Xue *et al.*, "Salidroside stimulates the Sirt1/PGC-1α axis and ameliorates diabetic nephropathy in mice," *Phytomedicine,* vol. 54, pp. 240–247, 2019.

54 T. Imasawa *et al.*, "High glucose repatterns human podocyte energy metabolism during differentiation and diabetic nephropathy," *FASEB J.,* vol. 31, no. 1, p. 294, 2016.

55 K. N. Miller, J. P. Clark, and R. M. Anderson, "Mitochondrial regulator PGC-1a—Modulating the modulator," *Curr. Opin. Endocr. Metab. Res.,* vol. 5, pp. 37–44, 2019.

56 G. Zhang, M. Darshi, and K. Sharma, "The Warburg effect in diabetic kidney disease," in *Semin. Nephrol.*, 2018, vol. 38, no. 2, pp. 111–120, 2018

57 S. Hasegawa and R. Inagi, "Harnessing metabolomics to describe the pathophysiology underlying progression in diabetic kidney disease," *Curr. Diabetes Rep.,* vol. 21, no. 7, p. 21, 2021.

58 J. Connors, N. Dawe, and J. Van Limbergen, "The role of succinate in the regulation of intestinal inflammation," *Nutrients,* vol. 11, no. 1, p. 25, 2018.

59 R. Bohuslavova, R. Cerychova, K. Nepomucka, and G. Pavlinkova, "Renal injury is accelerated by global hypoxia-inducible factor 1 alpha deficiency in a mouse model of STZ-induced diabetes," *BMC Endocr. Disord.,* vol. 17, pp. 1–12, 2017.

60 J. Liu *et al.*, "Hypoxia, HIF, and associated signaling networks in chronic kidney disease," *Int. J. Mol. Sci.,* vol. 18, no. 5, p. 950, 2017.

Abstract in Korean

당뇨병성 신장병에서 미토콘드리아 대사 보존을 위한 PGC−1α와 HIF−1α의 상관관계 규명

배경: 저산소유도인자−1α (HIF−1α)는 에너지 대사에서 다양한 역할을 하며, 여기에는 해당과정을 증가시키고, 피루브산 키네이스 M2(PKM2) 활성을 억제하는 것이 포함된다. 그러나 미토콘드리아 생합성의 주요 조절자인 퍼옥시좀 증식 활성화 수용체 감마 공동 조절자−1α (PGC−1α)와 HIF−1α 간의 상호작용은 아직 밝혀지지 않았다. 본 연구는 당뇨병 신증의 신세뇨관 상피 세포에서 PKM2 조절에 PGC−1α가 HIF−1α에 미치는 기전을 조사하는 것을 목표로 했다.

방법: C57BL/6 생쥐로부터 1 차 배양된 신세뇨관 상피 세포를 고혈당 상태에서 pPGC1α 또는 siPGC1α으로 자극했다. 또한 1 차 배양된 신세뇨관 상피 세포를 숙신산, siPGC1α, 또는 숙신산과 siPGC1α로 자극했다. 크로마틴 면역침전분석 및 루시퍼레이즈 분석을 수행하여 PGC−1α가 HIF−1α에 직접적인 조절 작용을 하는지 분석했다. 당뇨를 유도한 *db/db* 생쥐에게 메트포르민 또는 레스베라트롤을 12 주 동안 매일 경구 투약했으며 대조군으로 *db/m* 생쥐를 이용했다. 이후, TCA 회로 중간 대사물, PGC−1α, HIF−1α, PKM2 활성을 포함한 해당과정, 지방산 산화, 미토콘드리아 기능 및 형태를 조사했다.

결과: 고혈당 처리된 신세뇨관 상피 세포는 *Ppargc1a* 및 *Pkm2* 발현 감소, *Hif1a* 발현 증가, 비정상적인 해당과정 및 지방산 산화 장애를 보였다. 이러한 대사적 이상은 TCA 회로 중간 대사물인 숙산산의 축적을 초래했다. *Ppargc1a*의 과발현은 이러한 변화를 되돌렸고, *Ppargc1a*를 억제시키면 이러한 변화가 악화됐다. RTEC 에 숙산산을 처리하면 *Hif1a* 발현은 증가하고 *Pkm2* 발현은 감소했으며 비정상적인 해당과정이 유도됐다. 이러한 변화는 *Hif1a*를 침묵시킴으로써 완화됐다. 크로마틴 면역침전분석에서는 PGC−1α가 Hif−1α 유전자의 프로모터의 영역 내 HIF−1α 단백질의 결합영역 (hypoxia responsive element)에 직접 결합한다는 사실을 밝혔다. 숙산산 자극 하에서 PGC−1α의 HIF−1α에 대한 조절 작용은 억제되었고, *Ppargc1a*의 과발현에 의해 증가했다. 당뇨병 신장 질환 모델에서 메트포르민과 레스베라트롤로 유도된 *Ppargc1a* 활성화는 세포 실험 결과를 재현하였으며, 유리한 대사적 효과를 보였다.

결론: 당뇨병성 신증에서 PGC−1α 결핍은 TCA 회로 중간 대사물의 축적을 초래하고, 그 결과 HIF−1α 활성을 증가시키며 PKM2 활성을 감소시켰다. 또한 PGC−1α는 HIF−1α 활성을 직접적으로 억제하여 미토콘드리아 에너지 대사에서 중요한 조절 역할을 한다는 것을 밝혔다.

핵심되는 말: PGC−1α, HIF−1α, PKM2, TCA 회로, 신세뇨관 상피 세포, 당뇨병성 신장증